Journal of Medicinal Chemistry

pubs.acs.org/jmc Article

# Discovery of a Pyrimidinedione Derivative as a Potent and Orally Bioavailable Axl Inhibitor

Hefeng Zhang,[⊥] Xia Peng,[⊥] Yang Dai, Jingwei Shao, Yinchun Ji, Yiming Sun, Bo Liu, Xu Cheng, Jing Ai,* and Wenhu Duan*

Cite This: *J. Med. Chem.* 2021, 64, 3956−3975 Read Online

ACCESS | Metrics & More | Article Recommendations | Supporting Information

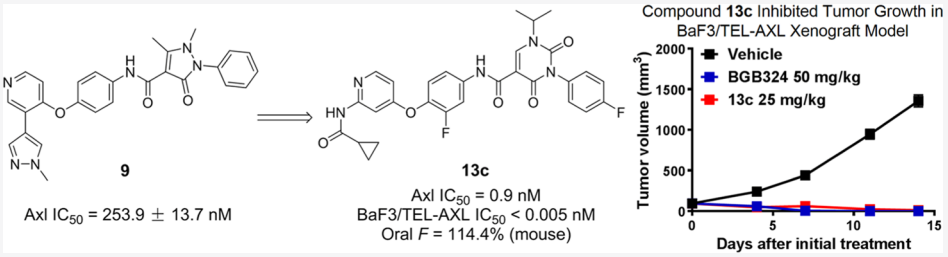


**ABSTRACT:** The receptor tyrosine kinase Axl plays important roles in promoting cancer progression, metastasis, and drug resistance and has been identified as a promising target for anticancer therapeutics. We used molecular modeling-assisted structural optimization starting with the low micromolar potency compound **9** to discover compound **13c**, a highly potent and orally bioavailable Axl inhibitor. Selectivity profiling showed that **13c** could inhibit the well-known oncogenic kinase Met with equal potency to its inhibition of Axl superfamily kinases. Compound **13c** significantly inhibited cellular Axl and Met signaling, suppressed Axl- and Met-driven cell proliferation, and restrained Gas6/Axl-mediated cancer cell migration or invasion. Furthermore, **13c** exhibited significant antitumor efficacy in Axl-driven and Met-driven tumor xenograft models, causing tumor stasis or regression at well-tolerated doses. All these favorable data make **13c** a promising therapeutic candidate for cancer treatment.

## INTRODUCTION

Axl is a receptor tyrosine kinase (RTK) that belongs to the TAM (Tyro3, Axl, and Mer) subfamily. Upon binding to its endogenous ligand growth arrest specific protein 6 (Gas6),[1] Axl dimerizes and gets autophosphorylated, resulting in the activation of downstream signaling pathways.[2−5] Gas6/Axl signaling regulates various biological processes, such as proliferation, differentiation, migration, apoptosis, angiogenesis, and immune response.[6,7]

Since the first identification of Axl in chronic myeloid leukemia (CML),[8] aberrant Axl signaling has been detected in many other cancers.[9−15] Overexpression of Axl closely correlates with poor prognosis.[3,16−21] Axl can heterodimerize with many other RTKs, including Met,[22−24] cooperating to promote tumor growth and metastasis. Moreover, Axl, as a key inducer of epithelial-to-mesenchymal transition (EMT), is potentially required for the metastatic feature of tumors, and blockading Axl could decrease tumor metastasis.[10,15,25−27] Recent evidence has shown the potential important regulatory role of Gas6/Axl in the interaction between cancer cells and stromal/immune cells in the tumor microenvironment, promoting tumor progression and metastasis.[28] Besides, Axl could mediate de novo and acquire resistance to chemotherapy, immunotherapy, molecular-targeted therapy, and radiation therapy.[21,26,29,30] Thus, targeting Axl is a promising strategy for anticancer therapeutics.

Several type I and type II ATP-competitive inhibitors that target Axl have been reported (Figure 1). Type I inhibitors such as **1** (gilteritinib)[31] and **2** (bemcentinib, BGB324)[32] bind to the active conformation of Axl, where the aspartate−phenylalanine−glycine (DFG) motif is oriented toward the ATP binding site. The potent FLT3/Axl inhibitor **1** has been approved by FDA to treat acute myeloid leukemia (AML) with FLT3 mutations. BGB324, which is disclosed as the first selective Axl inhibitor,[32] has advanced into phase I and II clinical trials against different types of cancers. Type II inhibitors bind to the inactive conformation of Axl, in which the DFG motif is oriented outward such that the protein could enable additional allosteric interactions. Compound **3** (cabozantinib)[33] is an FDA-approved multikinase inhibitor for treating various cancers, and the inhibitory potency of **3** against Axl is 200-fold less active than against VEGFR2.[34] Some other type II Axl

Received: December 3, 2020
Published: March 18, 2021







https://doi.org/10.1021/acs.jmedchem.0c02093
*J. Med. Chem.* 2021, 64, 3956−3975

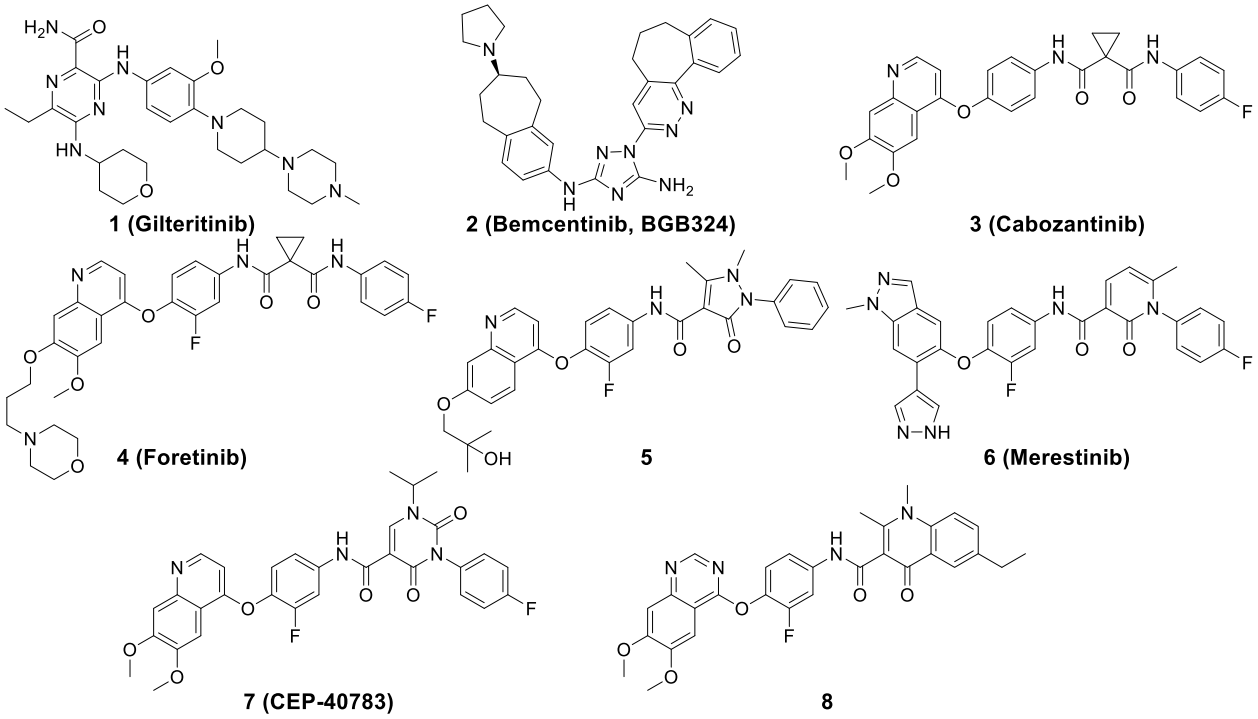


**Figure 1.** Chemical structures of representative Axl inhibitors.

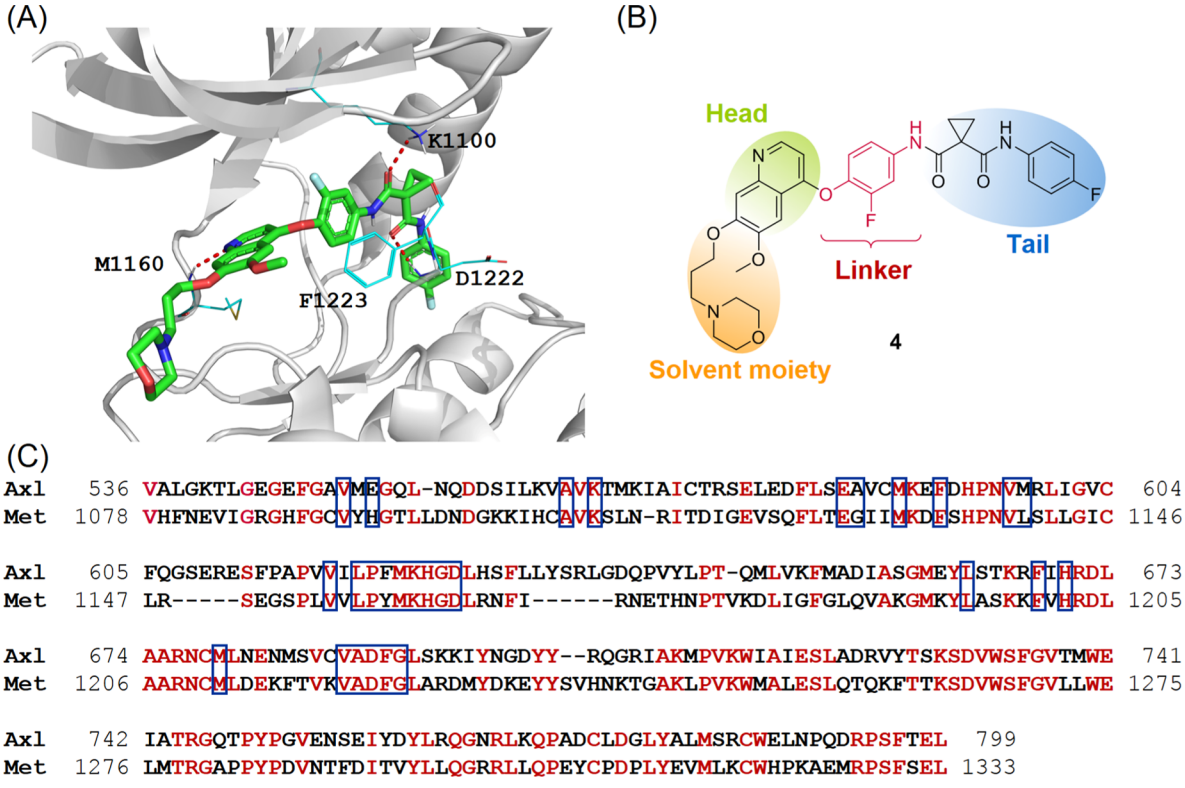


**Figure 2.** Analysis of the structural features of the type II Axl inhibitor from the cocrystal structure of Met in complex with the Axl inhibitor **4**: (A) binding mode of Met with the representative type II Axl inhibitor **4** (PDB ID: 3LQ8). (B) Compound **4** was used to display the structural features of classic type II Axl inhibitors. (C) Sequence alignment of Axl and Met kinase domains, where the identical residues are colored in red and the binding pocket residues of the Met DFG-out conformation are boxed.

inhibitors, such as **4** (foretinib),[35] **5**,[36] **6** (merestinib),[37] and **7** (CEP-40783),[38] are currently in different phases of clinical trials. Compound **8** is another potent type II Axl inhibitor with an $IC_{50}$ value of 4.0 nM.[39] The imaging probes derived from **8** have been successfully applied in proteome profiling and bioimaging of cancer cells and tumor tissues.[40]

Here, we describe the discovery of the orally active pyrimidinedione **13c** as a type II Axl inhibitor.



https://doi.org/10.1021/acs.jmedchem.0c02093
J. Med. Chem. 2021, 64, 3956−3975

## RESULTS AND DISCUSSION

**Design Rationale and Structure−Activity Relationship (SAR) Exploration.** A validated sandwich enzyme-linked immunosorbent assay (ELISA)[41] was used to determine the kinase inhibitory activities of new derivatives. Gilteritinib and BGB324 served as positive controls and displayed $IC_{50}$ values of 4.6 and 4.8 nM, respectively, which are consistent with previously reported data.[32,42] The classic gain-of-function model cell line BaF3/TEL-AXL was used to evaluate the antiproliferative effect of new derivatives.

No crystal structure is available for the Axl kinase domain in complex with a type II inhibitor to date. To elucidate the interactions between Axl and type II inhibitors, we obtained the Axl kinase domain sequence from the UniProt database (http://www.uniprot.org/) and performed a BLAST search (http://blast.ncbi.nlm.nih.gov) of the obtained sequence in the PDB database. The results demonstrated that except for the TAM subfamily members, Met had the highest sequence identity to the Axl kinase domain, with an identity value of 45.90%. In addition, 24 out of 28 residues in the DFG-out binding pocket of Met and Axl were identical (Figure 2C), which indicated that a type II inhibitor might bind to Met and Axl with similar binding modes. The binding mode of Met with the representative type II Axl/Met inhibitor **4** has been reported[35] (Figure 2A). It revealed that type II Axl inhibitors may have the following structural features: (1) a hinge-binding moiety "head", which is commonly a nitrogen-containing heterocycle as a hydrogen bond acceptor and may be decorated with substituents that stretch into the solvent region; (2) a "tail" containing a dual hydrogen bond acceptor (DHBA) segment and a hydrophobic aryl, where the active conformation of the tail moiety could be constrained by introducing a rigid ring; and (3) an aminophenoxyl linker that joins the head and the tail (Figure 2B). On the basis of this information, we initially designed and synthesized compound **9** (see Figure 3), which features a five-membered ring in the tail

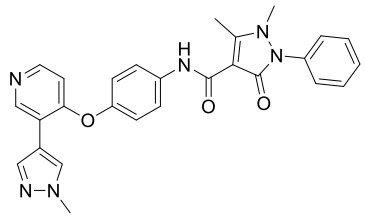


**9**
Axl $IC_{50}$ = 253.9 ± 13.7 nM
MW = 480.5

**Figure 3.** Chemical structure of compound **9**.

moiety for constraining the active conformation of the tail moiety and a flexible pyrazole-substituted pyridine in the head moiety. As a type II inhibitor, **9** also has a relatively low molecular weight (480.5) and has good potential for structural modification. Biochemical assays showed that compound **9** displayed moderate activity with an $IC_{50}$ value of 253.9 nM for Axl.

Our first step in optimizing the inhibitory potency of **9** involved the tail moiety. We adopted a hybrid design strategy by replacing the tail moiety of **9** with different known DHBA-containing fragments[39,43−49] to generate compounds **10a−n** (Table 1). Ethoxy-substituted pyrazole **10a** exhibited no activity on Axl, whereas pyrimidine-4-one **10b** displayed a significant increase in potency, with an $IC_{50}$ value of 20.5 nM for Axl. The installation of a methyl at the 6′-position of the pyrimidine-4-one moiety of **10b** led to a sharp loss in activity (**10c**), whereas replacement of pyrimidine-4-one of **10b** with pyrimidine-2,4-dione led to a slight increase in potency (**10d**, with an $IC_{50}$ of 13.0 nM). Given the improved potency of **10d**, variations at the 1′-position of the pyrimidine-2,4-dione fragment of **10d** were explored with four selected substituents to form compounds **10e−h**, among which ethyl and isopropyl substitutions led to a slight increase in potency with $IC_{50}$ values of 8.8 and 8.7 nM for **10f** and **10g**, respectively. Replacing pyrimidine-2,4-one with its bioisoster 1,2,4-triazine-3,5-dione resulted in a sharp drop in potency (**10i**). We also synthesized a set of compounds featuring fused heterocyclic moieties (**10j−n**); replacement of the tail moiety with 7,8-dihydroquinoline-2,5-dione and 1,7-naphthyridin-2-one moieties led to improved activities (**10l** and **10m** vs **9**), whereas replacement with the inden-1-one moiety (**10j**), 6,7-dihydroisoquinoline-3,8-dione moiety (**10k**), and quinolin-4-one moiety (**10n**) led to a complete loss of activity. As a result, **10g** was identified as the optimal compound for further investigation.

A better understanding of the binding mode of **10g** with Axl could pave the way for further rational design; therefore, we carried out an in silico molecular modeling study. As mentioned above, there is no available crystal structure for Axl in complex with a type II inhibitor, and Met has the highest sequence identity to the Axl kinase domain; in addition, 24 out of 28 residues in the DFG-out binding pocket of Met and Axl are identical (Figure 2C); thus, a Met DFG-out crystal structure can serve as a template for generating an Axl DFG-out homology model. We first constructed an Axl DFG-out homology model based on a reported DFG-out Met kinase crystal structure (PDB ID: 3F82).[50] The predicted Axl DFG-out homology model was highly similar to the Met crystal structure in both the overall folding and binding pockets (Figure S1). Next, we docked **10g** to the Axl DFG-out model. The result showed that **10g** adopted a canonical type II binding mode and could fit well into the DFG-out pocket (Figure 4). The tail moiety occupied the allosteric binding site, and the DHBA fragment formed two hydrogen bonds with residues Lys567 and Asp690. The isopropyl and 4-fluorophenyl stretched to two different hydrophobic pockets. A critical hydrogen bond was formed in the hinge region between the nitrogen atom of the pyridine moiety and the backbone NH of the residue Met623. The aminophenoxyl moiety acted as a linker and occupied the hydrophobic tunnel. This simulated result provided useful information for further rational design: (1) as the 1-methyl pyrazole moiety of **10g** did not present strong interactions with the binding pocket, we envisioned that shifting this moiety to the ortho-position of the pyridine nitrogen might allow the inhibitor to approach the pocket surface more closely to enhance van der Waals interactions; (2) the hydrophobic tunnel occupied by the aminophenoxyl linker could only tolerate small substituents; and (3) the carbonyl oxygen of Met623 might be a potential hydrogen bond acceptor, and the potency could presumably be improved by installing an additional hydrogen bond donor at the ortho-position of the pyridine nitrogen.

First, the effect of shifting the 1-methyl pyrazole moiety to the ortho-position of the pyridine nitrogen was examined, and the result showed that *ortho*-pyrazole-substituted pyridine **11a** ($IC_{50}$: 1.9 nM) exhibited a significant increase in potency compared to its metasubstituted analogue **10g** ($IC_{50}$: 8.7 nM), as shown in Table 2. Then, selected SAR from substitution on the aminophenoxyl linker is summarized as in Table 2. Fluoro


https://doi.org/10.1021/acs.jmedchem.0c02093
J. Med. Chem. 2021, 64, 3956−3975

**Table 1. SAR of the Tail Moiety**[a]

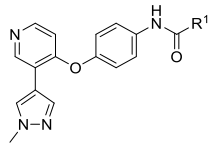

| Compds | $R^1$ | Axl Kinase Inhibitory $IC_{50}$ (nM) | Compds | $R^1$ | Axl Kinase Inhibitory $IC_{50}$ (nM) |
|---|---|---|---|---|---|
| 9 | 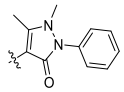 | 253.9 ± 13.7 | 10i | 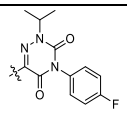 | 178.6 ± 18.6 |
| 10a | 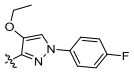 | >1000 | 10j | 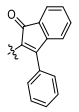 | >1000 |
| 10b | 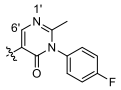 | 20.5 ± 4.6 | 10k | 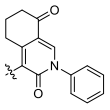 | >1000 |
| 10c | 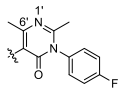 | 395.7 ± 21.3 | 10l | 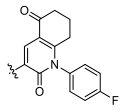 | 16.8 ± 1.4 |
| 10d | 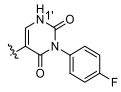 | 13.0 ± 2.5 | 10m | 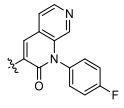 | 150.0 ± 17.5 |
| 10e | 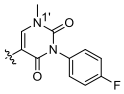 | 184.8 ± 8.1 | 10n | 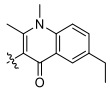 | >1000 |
| 10f | 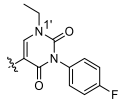 | 8.8 ± 2.1 | 1 | | 4.6 ± 0.6 |
| 10g | 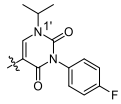 | 8.7 ± 5.0 | 2 | | 4.8 ± 0.8 |
| 10h | 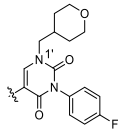 | 58.3 ± 4.2 | | | |

[a]The Axl kinase inhibitory $IC_{50}$ values are the mean ± SD of two or more independent assays or estimated values.

substitution is more favorable at the $R^2$-position than at the $R^3$-position ($IC_{50}$: 0.8 nM for **11b** vs 5.5 nM for **11c**). Chloro and methyl substitutions resulted in 27- and 57-fold decreases in potency for **11d** and **11e**, respectively. Methoxy substitution, as in **11f**, resulted in a complete loss of activity. Difluoro-substituted derivatives **11g**, **11h**, and **11i** displayed a slight decrease in potency compared to the monofluoro derivative **11b**. The monofluoro derivative **11b** represented the optimal substitution pattern on the aminophenoxyl linker, and the narrow SAR is consistent with expectations, given the limited space available for the linker in this region.

We next explored the effect of substituents on the pyrazole fragment (Table 3). The introduction of a methyl group at the $R^5$-position (**12a**) resulted in a 32-fold loss in potency for Axl kinase, while a slight increase in cellular potency (BaF3/TEL-AXL $IC_{50}$: 1 nM for **12a** vs 1.9 nM for **11b**). The derivatives substituted with three selected larger groups at the $R^6$-position (**12b–d**) were less active than the methyl-substituted derivative **11b** in both enzymatic and cellular assays. According to the concept of "heteroatom release",[51] the group on the heteronitrogen atom, as the methyl group in **11b** at the $R^6$-position, is potentially metabolically labile; consequently, a methyl-free compound **12e** was synthesized. Compound **12e** displayed a slight decrease in potency for kinase inhibitory activity, but significantly improved potency in the BaF3/TEL-AXL assay ($IC_{50}$ < 0.2 nM). On account of their in vitro potencies and metabolic labile site, compound **12e** was identified as the optimal pyrazole derivatives.

Finally, we attempted to add an additional hydrogen bond donor at the ortho-position of the pyridine fragment, as


https://doi.org/10.1021/acs.jmedchem.0c02093
J. Med. Chem. 2021, 64, 3956−3975

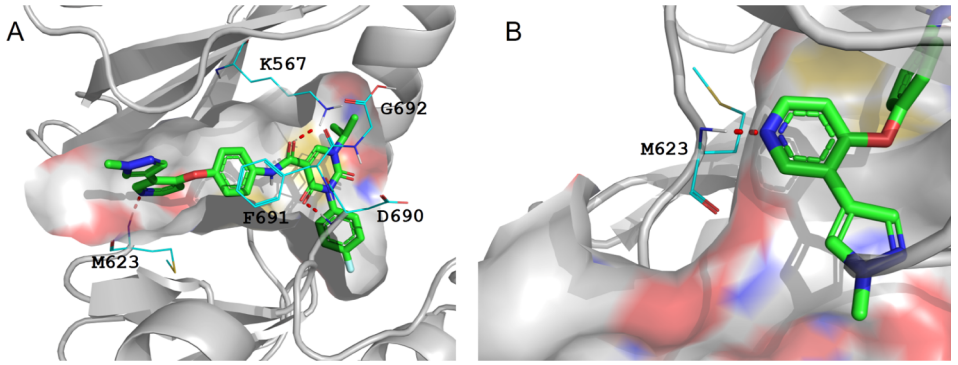


**Figure 4.** Schematic illustration of the proposed binding mode of **10g** with the Axl DFG-out homology model (generated from PDB ID: 3F82): (A) Type II binding model of compound 10**g**. (B) Compound **10g** with the hinge region.

**Table 2. SAR of the Linker Moiety 11a−i**[a]

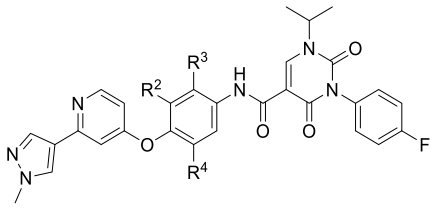

| compds | $R^2$ | $R^3$ | $R^4$ | Axl kinase inhibitory $IC_{50}$ (nM) |
|---|---|---|---|---|
| **11a** | H | H | H | 1.9 ± 0.6 |
| **11b** | F | H | H | 0.8 ± 0.3 |
| **11c** | H | F | H | 5.5 ± 1.6 |
| **11d** | Cl | H | H | 21.9 ± 0.9 |
| **11e** | Me | H | H | 45.6[b] |
| **11f** | OMe | H | H | >1000 |
| **11g** | F | F | H | 4.9 ± 1.0 |
| **11h** | H | F | F | 2.75 ± 0.5 |
| **11i** | F | H | F | 3.7 ± 0.2 |
| **1** | | | | 4.6 ± 0.6 |
| **2** | | | | 4.8 ± 0.8 |

[a]Unless otherwise specified, the Axl kinase inhibitory $IC_{50}$ values are the mean ± SD of two or more independent assays or estimated values. [b]The result is obtained from a single assay.

indicated in the docking studies, to form bidentate hydrogen bonds with Met623 in the hinge region of Axl. The results showed that replacement of the pyrazole fragment with amide or urea fragments was successful; as summarized in Table 4, almost all new derivatives displayed high potency in both enzymatic and cellular assays, with the exception of **13d**, which showed moderate cellular activity. The most potent compound **13c** was docked to the Axl DFG-out homology model, as shown in Figure 5, and **13c** shared the same allosteric interactions with **10g** and formed bidentate hydrogen bonds with Met623 at the hinge region as expected.

**Pharmacokinetic Study.** Compounds **12e** and **13c** were chosen for in vivo pharmacokinetic studies because of their excellent enzymatic and cellular activities. Preliminary pharmacokinetic evaluations were conducted in male Sprague−Dawley (SD) rats. The pharmacokinetic parameters are summarized in Table 5. Both compounds displayed good maximum concentrations and oral exposures; **13c** had a favorable half-life of 13.8 h, whereas compound **12e** exhibited a long half-life of 18.2 h, which may bring about a potential risk of cumulative toxicity. Consequently, compound **13c** was selected for subsequent pharmacokinetics assessment in male Institute of Cancer Research (ICR) mice. Table 6 shows the good pharmacokinetic parameters displayed by **13c** in the ICR mice.

**Table 3. SAR of the Pyrazole Fragment**[a]

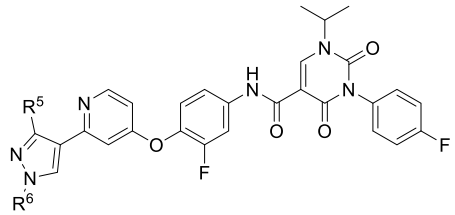

| | | | inhibitory $IC_{50}$ (nM) | |
|---|---|---|---|---|
| compds | $R^5$ | $R^6$ | Axl kinase | BaF3/TEL-AXL proliferation |
| **11b** | H | Me | 0.8 ± 0.3 | 1.9 ± 0.4 |
| **12a** | Me | Me | 25.6 ± 4.5 | 1.0 ± 0.4 |
| **12b** | H | Cyclopropyl | 10.5 ± 1.1 | 6.3 ± 0.2 |
| **12c** | H | 2-hydroxy-2-methylpropyl | 17.4 ± 6.2 | 2.8 ± 1.6 |
| **12d** | H | 2-(4-methylpiperazin-1-yl)ethyl | 26.0 ± 3.1 | 19.5 ± 8.9 |
| **12e** | H | H | 3.1 ± 0.3 | <0.2 |
| **1** | | | 4.6 ± 0.6 | 7.6 ± 4.9 |
| **2** | | | 4.8 ± 0.8 | 117.2 ± 8.1 |

[a]The $IC_{50}$ values are the mean ± SD of two or more independent assays or estimated values.



https://doi.org/10.1021/acs.jmedchem.0c02093
J. Med. Chem. 2021, 64, 3956−3975

**Table 4. Axl Inhibitory Activities of Inhibitors 13a−e[a]**

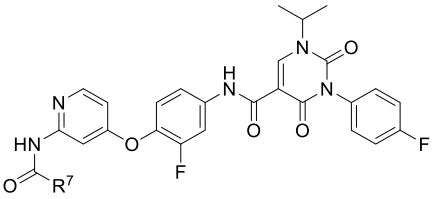

| compds | $R^7$ | inhibitory $IC_{50}$ (nM) | |
|---|---|---|---|
| | | Axl kinase | BaF3/TEL-AXL proliferation |
| **13a** | Me | 6.7 ± 0.3 | <0.2 |
| **13b** | Et | 5.8 ± 1.1 | <0.2 |
| **13c** | cyclopropyl | 0.9 ± 0.1 | <0.005 |
| **13d** | cyclobutyl | 8.0 ± 0.9 | 43.2 ± 1.8 |
| **13e** | pyrrolidin-1-yl | 1.7 ± 0.2 | <0.2 |
| **13f** | morpholino | 8.6 ± 2.8 | <0.2 |
| **1** | | 4.6 ± 0.6 | 7.6 ± 4.9 |
| **2** | | 4.8 ± 0.8 | 117.2 ± 8.1 |

[a]The $IC_{50}$ values are the mean ± SD of two or more independent assays or estimated values.

**Table 5. Pharmacokinetic Data of 12e and 13c in Rats[a]**

| parameter | 12e po 3 mg/kg | 13c po 3 mg/kg |
|---|---|---|
| $AUC_{0-t}$ (ng·h/mL) | 31,641 | 32,647 |
| $AUC_{0-\infty}$ (ng·h/mL) | 52,165 | 43,931 |
| $T_{1/2}$ (h) | 18.2 | 13.8 |
| $T_{max}$ (h) | 1.67 | 1.17 |
| $C_{max}$ (ng/mL) | 2573 | 4557 |

[a]Three animals were used for each dose group. The data shown are mean values.

**Table 6. Pharmacokinetic Data of 13c in Mice[a]**

| parameter | 13c po 3 mg/kg | 13c iv 1 mg/kg |
|---|---|---|
| $AUC_{0-t}$ (ng·h/mL) | 24,044 | 7006 |
| $AUC_{0-\infty}$ (ng·h/mL) | 25,106 | 7356 |
| $T_{1/2}$ (h) | 5.20 | 5.57 |
| $T_{max}$ (h) | 1.67 | |
| $C_{max}$ (ng/mL) | 2990 | |
| CL (mL/h/kg) | | 2.29 |
| *F* % | 114.4 | |

[a]Three animals were used for each group. The data are mean values.

**Kinase Selectivity Profile of 13c.** The kinase selectivity of **13c** was further evaluated over a panel of 41 kinases, including the TAM subfamily members Mer and Tyro3 and the highly homologous kinase Met. Compound **13c** also significantly inhibited the kinases activity of Mer, Tyro3, and Met. The potency of **13c** against Met was equal to that against Axl (Met $IC_{50}$: 0.8 ± 0.1 nM). In contrast, no obvious inhibitory effect was observed in the other 38 tested tyrosine kinases belonging to different families ($IC_{50}$ > 1 μM or 100 nM) (Table 7). These results indicated that **13c** was a potent TAM and Met inhibitor. Next, we used representative Axl- and Met-driven in vitro and in vivo scenarios to evaluate the antitumor effect of **13c** against Axl and Met.

**Compound 13c Inhibited Cellular Axl and Met Signaling.** We evaluated the cellular effects of **13c** against Axl and Met signaling for Axl-driven or Met-dependent scenarios, respectively. First, the classic gain-of-function model cell BaF3/TEL-AXL, in which proliferation is driven by *AXL* fusion, was used. Treatment with **13c** led to a robust decrease in the phosphorylation of Axl and its key downstream molecule Akt[10] in BaF3/TEL-AXL cells (Figure 6A). Furthermore, we extended to Gas6-stimulated Axl activation context. The nonsmall cell lung cancer cell line NCI-H1299 is sensitive to Gas6 stimulation, as evidenced by the markedly enhanced phosphorylation of Axl and the downstream molecule Akt. Treatment with **13c** inhibited the Gas6-induced upregulation of Axl and Akt phosphorylation. The activity of **13c** was more potent than that of BGB324 (Figure 6B). Next, we determined whether **13c** could inhibit the Met signaling pathway in the Met-driven context using MKN45 and EBC-1 cells, both with *MET* amplification. The reported Met inhibitor crizotinib[52] served as a positive control. As shown, **13c** suppressed the phosphorylation of Met and downstream signaling molecules of Met (ERK and Akt) in a dose-dependent manner (Figure 6C,D). These data demonstrated that **13c** inhibited both cellular Axl and Met signaling pathways.

**Compound 13c Restrained Axl/Met-Driven Cell Proliferation with Selectivity.** Table 4 shows that **13c** exhibited high potency against Axl-mediated cell proliferation. Given the activity of **13c** against c-Met kinase, we next evaluated the activity of **13c** against EBC-1 and MKN45 cell proliferation driven by *MET* amplification. Compound **13c** inhibited the proliferation of MKN45 and EBC-1 cells with $IC_{50}$ values of 64.0 ± 5.4 and 106.8 ± 19.4 nM, respectively.

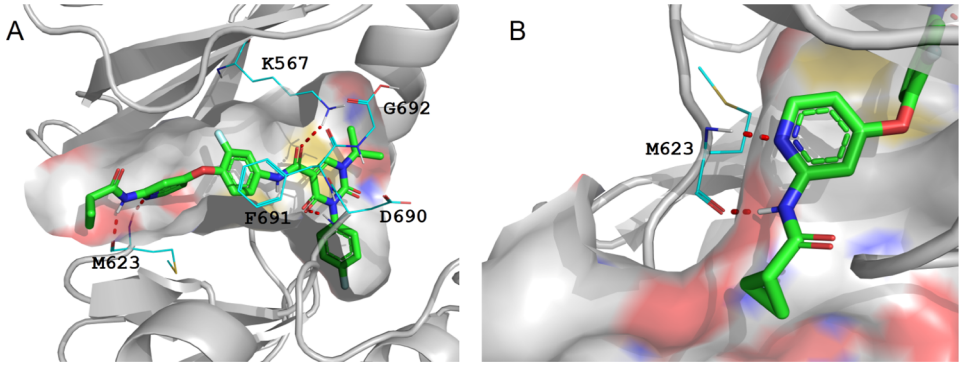


**Figure 5.** Schematic illustration of the proposed binding mode of **13c** with the Axl DFG-out homology model (generated from PDB ID: 3F82): (A) Type II binding model of compound **13c**. (B) Compound **13c** with the hinge region.



https://doi.org/10.1021/acs.jmedchem.0c02093
J. Med. Chem. 2021, 64, 3956−3975

**Table 7. Kinase Selectivity Profile of 13c**[a]

| kinase | inhibitory $IC_{50}$ (nM) | kinase | inhibitory $IC_{50}$ (nM) | kinase | inhibitory $IC_{50}$ (nM) |
|---|---|---|---|---|---|
| Axl | 0.9 ± 0.1 | HER4(ErbB4) | >1000 | mTOR | >1000 |
| Met | 0.8 ± 0.1 | Src | >1000 | PKA | >1000 |
| Mer | <10 | Abl | >1000 | Ret | >1000 |
| Tyro3 | 1−10 | EphA2 | >100 | p90RSK | >1000 |
| ALK | >1000 | IGF1R | >1000 | Syk | >100 |
| FGFR1 | >1000 | A-Raf | >1000 | ZAK | >100 |
| VEGFR1 | >1000 | BTK | >1000 | CaMK1 | >1000 |
| VEGFR2 | >1000 | CLK1 | >1000 | CDK1/cyclinB | >1000 |
| PDGFR$\alpha$ | >1000 | FAK | >1000 | CDK2/cyclinA | >1000 |
| PDGFR$\beta$ | >1000 | GCK | >1000 | CDK4/cyclinD3 | >1000 |
| Kit | >1000 | JAK1 | >1000 | CDK6/cyclinD3C | >1000 |
| Flt-1 | >1000 | JAK3 | >1000 | CDK12/cyclinK | >1000 |
| Flt-3 | >1000 | ERK2 | >1000 | PI3K(p110d/p85a) | >1000 |
| EGFR | >1000 | MEK1 | >1000 | | |

[a]The $IC_{50}$ values are presented as the mean ± SD or estimated values.

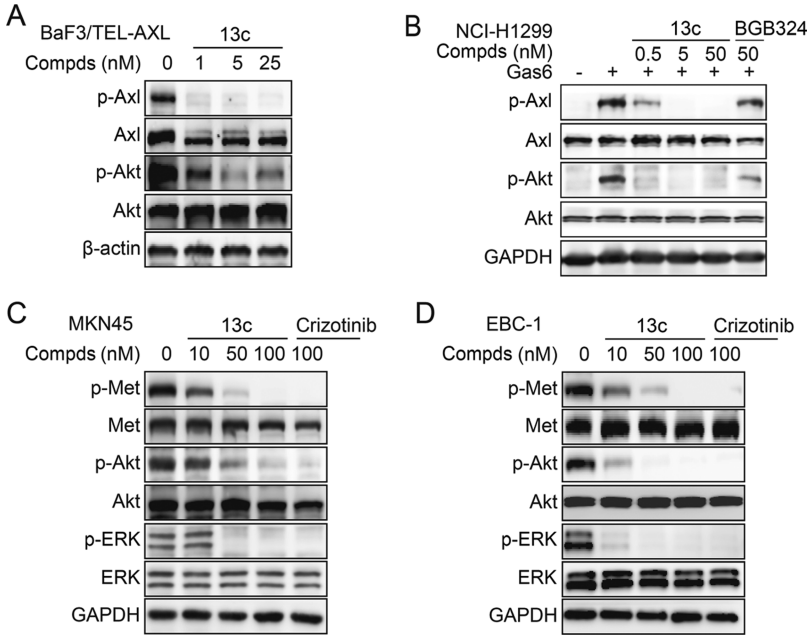


**Figure 6.** Compound **13c** suppressed Axl/Met phosphorylation and downstream signaling in BaF3/TEL-AXL cells (A), NCI-H1299 cells (B), MKN45 cells (C), and EBC-1 cells (D). BaF3/TEL-AXL, MKN45, and EBC-1 cells were treated with compounds at different concentrations for 2 h; NCI-H1299 cells were serum-deprived for 24 h prior to 2 h of treatment with compounds and then stimulated with Gas6 for 15 min. Then, the cells were lysed and subjected to western blot analysis.

Furthermore, we extended to 14 other cancer cell lines without *MET* or *AXL* aberrations. We found that **13c** exerted little antiproliferative effect in these cell lines ($IC_{50}$ > 10 $\mu$M, see Table 8). The cell line inhibitory profile results, together with the biochemical kinase profile results, confirmed that **13c** selectively inhibited Axl/Met.

**Compound 13c Attenuated Gas6/Axl-Mediated Cancer Cell Migration and Invasion.** Given the critical role of Axl in the tumor metastatic phenotype, we evaluated the effect of **13c** on Gas6/Axl axis-mediated tumor cell migration and invasion. A cell migration assay using NCI-H1299 cells was first performed. Gas6 stimulation strongly enhanced the motility of NCI-H1299 cells, whereas **13c** markedly decreased the NCI-H1299 cell motility induced by Gas6. We observed a similar trend in the cell invasion assay. The invasion of the SNU449 cell line was enhanced by the addition of Gas6. Treatment with **13c** inhibited cell invasion (Figure 7). The activity of **13c** was more potent than that of BGB324. In addition, **13c** showed no effect on cell proliferation under the same conditions (data not shown), largely excluding the possibility that the inhibitory effect of **13c** on cell movement was caused by inhibition of cell proliferation. Therefore, **13c** could inhibit the motility of cancer cells driven by the activation of the Axl pathway in vitro, indicating the therapeutic potential of **13c** for tumor metastasis.

**Compound 13c Inhibited Axl-Driven or Met-Driven Tumor Growth In Vivo.** We investigated the antitumor activity of **13c** in vivo against established xenograft models derived from BaF3/TEL-AXL. Once the tumor volume reached 150−200 $mm^3$, tumor-bearing BALB/c nude mice were randomly assigned to five groups and treated with a vehicle or the indicated compound for 14 consecutive days. Figure 8A shows that **13c** significantly suppressed tumor growth. The tumor growth inhibition (TGI) rates of **13c** were 106.4, 105.9, and 90.9% at doses of 25, 5, and 1 mg/kg, respectively; four out of six


https://doi.org/10.1021/acs.jmedchem.0c02093
J. Med. Chem. 2021, 64, 3956−3975

**Table 8. Cell Line Proliferation Inhibitory and Selectivity Profile of 13c**[a]

| cell line | inhibitory $IC_{50}$ (nM) |
|---|---|
| BT474 | >10,000 |
| HCC78 | >10,000 |
| JHH7 | >10,000 |
| MDA-MB-231 | >10,000 |
| NCI-H1975 | >10,000 |
| NCI-H1299 | >10,000 |
| HT29 | >10,000 |
| HCC827 | >10,000 |
| BT549 | >10,000 |
| KMS11 | >10,000 |
| RT112 | >10,000 |
| MM.1S | >10,000 |
| HL60 | >10,000 |
| HCC4006 | >10,000 |

[a]The $IC_{50}$ values are estimated values.

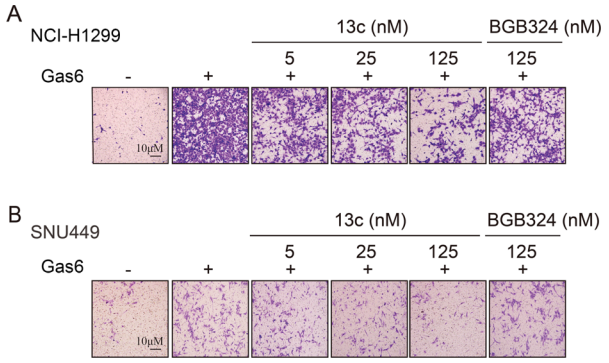


**Figure 7.** Compound **13c** inhibited Axl-dependent neoplastic phenotypes of metastasis: (A) Compound **13c** suppressed Gas6-induced NCI-H1299 cell migration. (B) Compound **13c** inhibited Gas6-induced SNU449 cell invasion. Representative images are shown (scale bars, 10 $\mu$m).

mice exhibited complete tumor regression in both the 25 and 5 mg/kg treatment groups. The efficacy of 5 mg/kg **13c** was comparable to that of 50 mg/kg BGB324. These results indicated that **13c** is a potent Axl inhibitor with potential for further development. Encouraged by the high activity of **13c** to reverse the Met-dependent tumor phenotype in vitro, we evaluated the antitumor efficacy of **13c** in vivo. The U87MG model driven by dysregulation of Met was used. Compound **13c** significantly inhibited tumor growth of the U87MG model in a dose-dependent manner, where the TGI rates of 100, 25, and 5 mg/kg were 99.1, 89.8, and 62.3% respectively (Figure 8B). Additionally, **13c** was well tolerated, with no substantial body weight loss in all the treated groups, even at the highest dose of 100 mg/kg (data not shown).

**Chemistry.** The syntheses of **9** and **10a−n** are illustrated in Scheme 1. The starting compound 3-chloro-4-bromopyridine (**14**) was reacted with 4-aminophenol to provide **15**. Suzuki coupling of **15** with 1-methyl-4-pyrazole boronic acid pinacol ester afforded amine **16**, which was condensed with acids **17a−o** to produce amides **9** and **10a−n**.

The syntheses of **11a−g**, **11i**, and **12a−e** were similar to those described for **9**, as illustrated in Scheme 2. The reaction of 2,4-dichloropyridine (**18**) with various 4-aminophenols produced **19a−h**, which were further coupled with different boronic acid pinacol esters to afford amines **20a−m**. Condensation of **20a−m** with **17h** provided **11a−g**, **11i**, and **12a−e**.

Compound **11h** was synthesized according to the procedures outlined in Scheme 3. The starting compound 2-chloro-4-hydroxypyridine (**21**) was reacted with 1,2,4-trifluoro-5-nitrobenzene, and the resulting nitrobenzene **22** was then reduced to provide amine **23**, which was reacted with 1-methyl-4-pyrazole boronic acid pinacol ester by Suzuki coupling to afford amine **24**. Finally, acid **17h** was condensed with amine **24** to produce **11h**.

Compounds **13a−c** were synthesized according to the procedures outlined in Scheme 4. Amine **25** was condensed with appropriate acid chlorides, and the resulting amides **26a−c** were then reacted with 2-fluoro-4-nitrophenol to afford nitro compounds **27a−c**, which were reduced to amines **28a−c** with iron powder. Amines **28a−c** were condensed with acid **17h** to yield **13a−c**.

Compounds **13d−f** were synthesized according to the procedures outlined in Scheme 5. 4-Chloropicolinamide (**29**) was reacted to yield amine **30**, which was then condensed with acid **17h** to afford amide **31**. Amide **31** was converted to amine **32** by a Hoffman rearrangement reaction. Compound **13d** was synthesized by coupling amine **32** with cyclobutane carboxylic acid. Compounds **13e** and **13f** were synthesized by reaction of **32** with pyrrolidine and morpholine, respectively.

## CONCLUSIONS

In summary, we designed and synthesized a series of Axl inhibitors of the type II class. Molecular modeling-assisted optimization led to the identification of **13c**, which was highly potent in both biochemical and cellular assays (Axl $IC_{50}$: 0.9 nM,

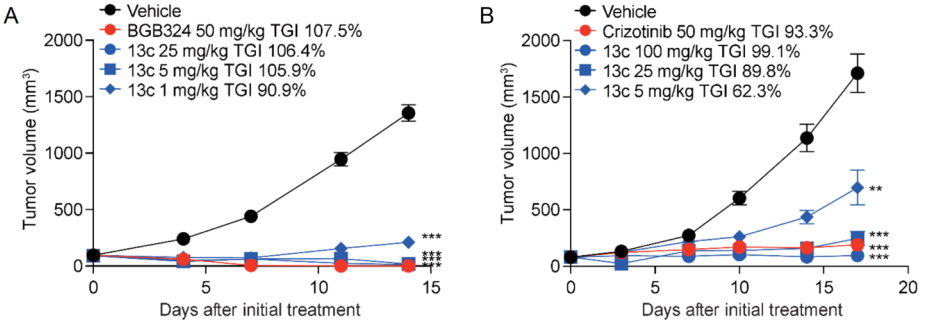


**Figure 8.** Compound **13c** significantly inhibited Axl/Met-mediated tumor growth in vivo: (A) Tumor growth was inhibited after **13c** treatment in BaF3/TEL-AXL xenografts. (B) Tumor growth was inhibited after **13c** treatment in U87MG xenografts. The tumor volumes are expressed as the mean ± SEM. Significant differences from the vehicle group were determined using a *t*-test, ***$P < 0.001$ and **$P < 0.01$.



https://doi.org/10.1021/acs.jmedchem.0c02093
J. Med. Chem. 2021, 64, 3956−3975

**Scheme 1. Syntheses of 9 and 10a−n**[a]

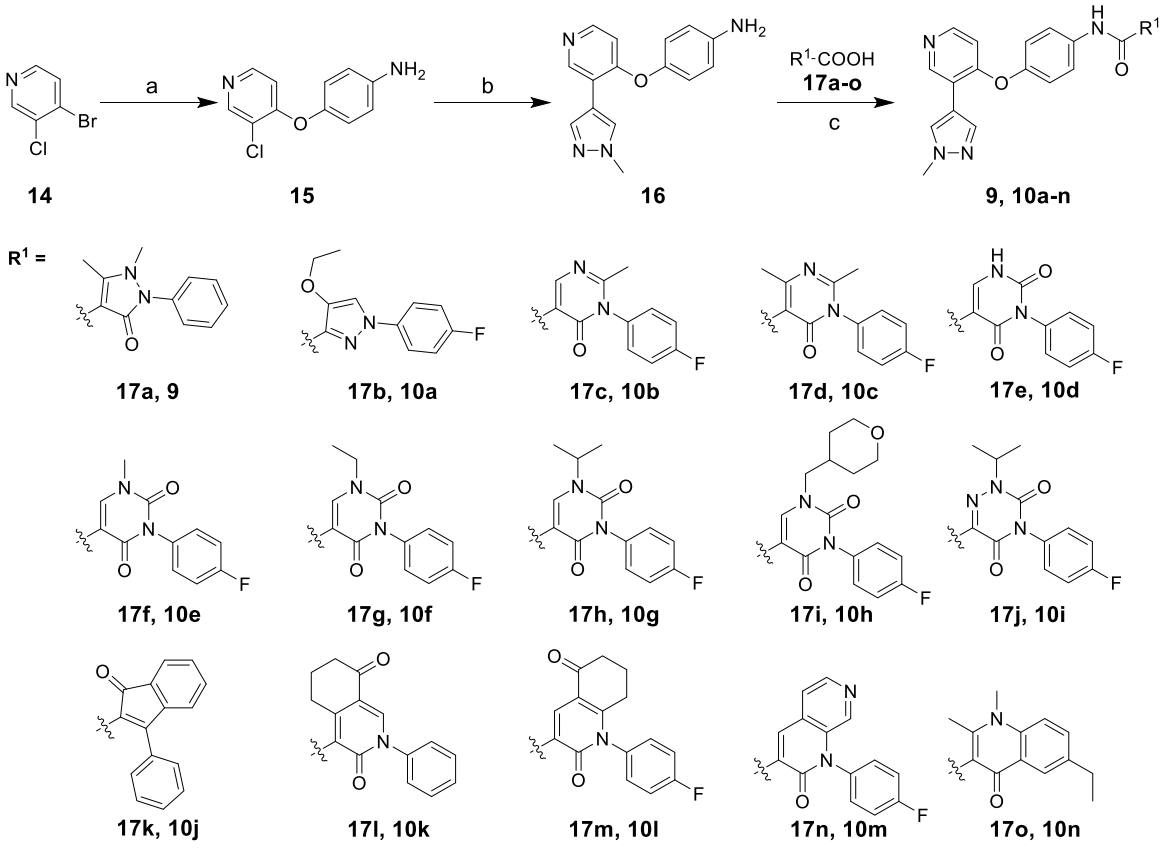


[a]Reagents and conditions: (a) 4-aminophenol, potassium *tert*-butoxide, dimethylacetamide (DMA), room temperature (RT) to 85 °C; (b) 1-methyl-4-pyrazole boronic acid pinacol ester, $Pd(PPh_3)_4$, 1,4-dioxane/water, 90 °C; and (c) *O*-(7-aza-1*H*-benzotriazol-1-yl)-*N*,*N*,*N*′,*N*′-tetramethyluronium hexafluorophosphate (HATU), triethylamine (TEA), *N*,*N*-dimethylformamide (DMF), RT.

**Scheme 2. Syntheses of 11a−g, 11i, and 12a−e**[a]

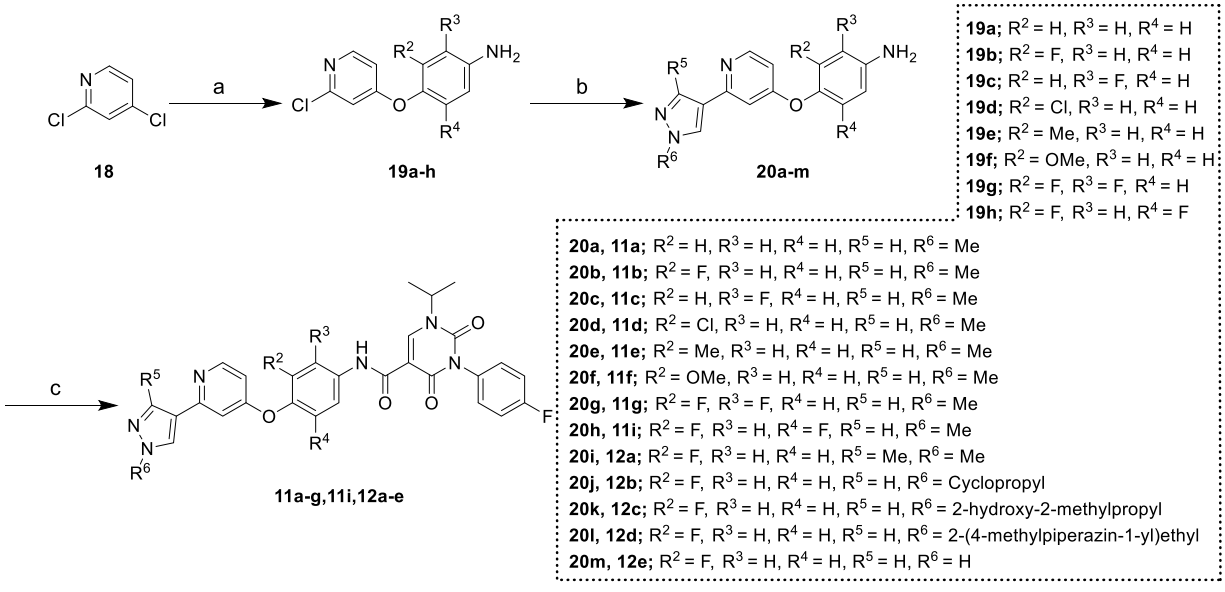


[a]Reagents and conditions: (a) appropriate 4-aminophenol, potassium *tert*-butoxide, DMA, RT to 85 °C; (b) 1-methyl-4-pyrazole boronic acid pinacol ester, $Pd(PPh_3)_4$, 1,4-dioxane/water, 90 °C; and (c) acid **17h**, HATU, TEA, DMF, RT.

BaF3/TEL-AXL $IC_{50}$ < 0.005 nM). Compound **13c** displayed good pharmacokinetic parameters in both rats and mice. Further evaluation revealed that **13c** exhibited kinase selectivity for TAM subfamily members and the homologous kinase Met. Compound **13c** significantly suppressed cellular Axl and Met signaling and inhibited the proliferation of cells driven by *AXL*-



https://doi.org/10.1021/acs.jmedchem.0c02093
J. Med. Chem. 2021, 64, 3956−3975

**Scheme 3. Synthesis of 11h**[a]

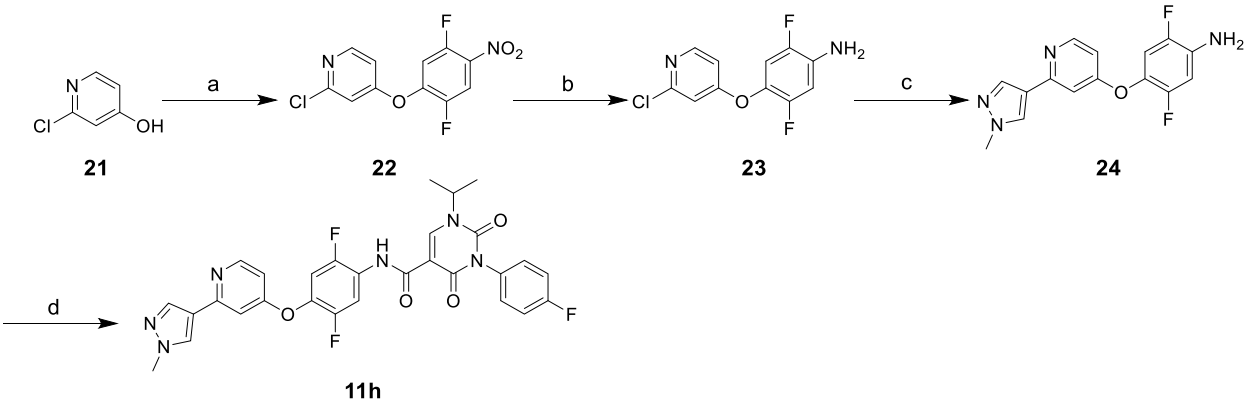


[a]Reagents and conditions: (a) $K_2CO_3$, 1,2,4-trifluoro-5-nitrobenzene, DMF, RT; (b) $SnCl_2$, EtOH, 80 °C; (c) 1-methyl-4-pyrazole boronic acid pinacol ester, $Pd(PPh_3)_4$, 1,4-dioxane/water, 90 °C; and (d) acid **17h**, HATU, TEA, DMF, RT.

**Scheme 4. Syntheses of 13a−c**[a]

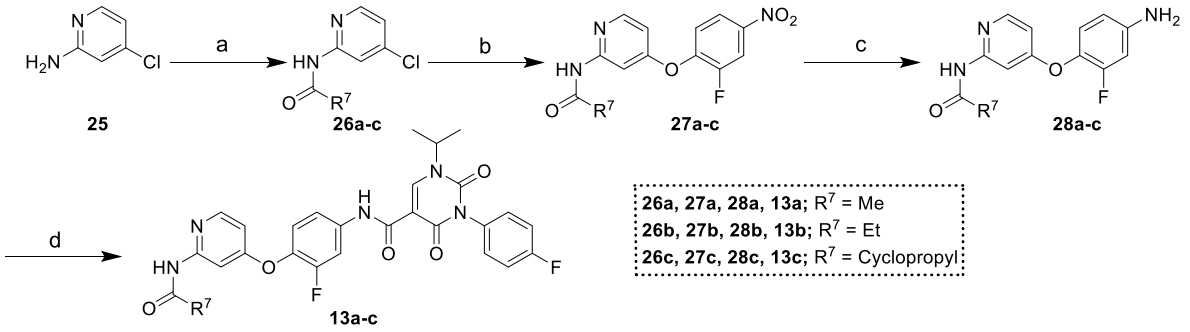


[a]Reagents and conditions: (a) appropriate acid chloride, TEA, dichloromethane, 0 °C to RT; (b) 2-fluoro-4-nitrophenol, chlorobenzene, 140 °C; (c) iron powder, acetic acid, ethyl acetate, 80 °C; and (d) acid **17h**, HATU, TEA, DMF, RT.

**Scheme 5. Syntheses of 13d−f**[a]

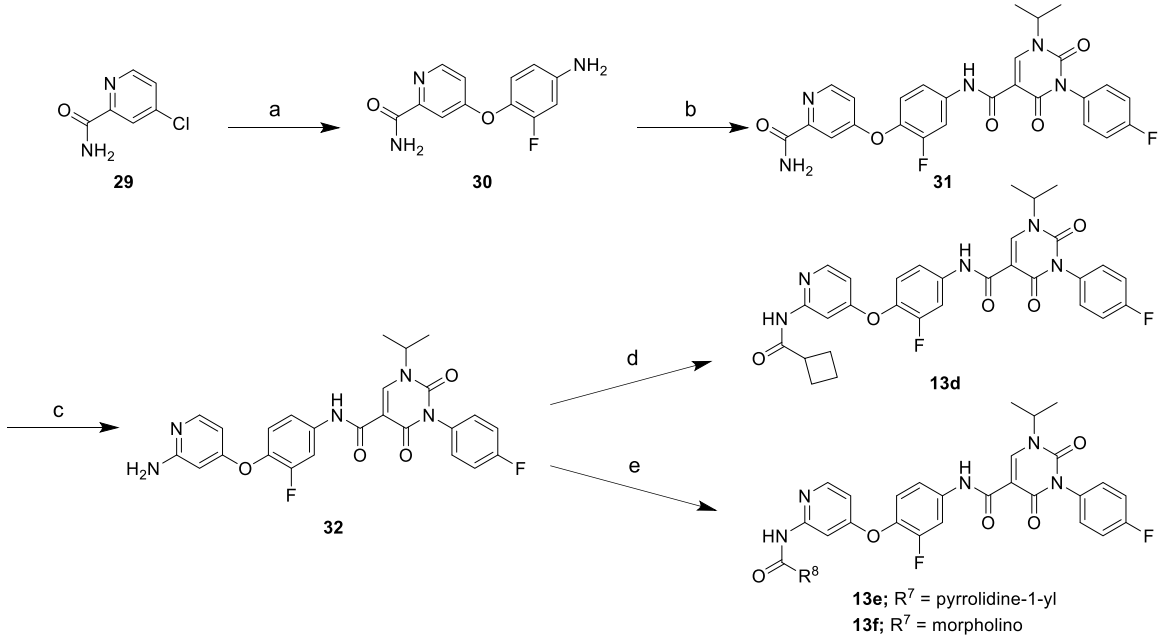


[a]Reagents and conditions: (a) 4-amino-2-fluorophenol, potassium *tert*-butoxide, dimethyl sulfoxide (DMSO), RT to 80 °C; (b) acid **17h**, HATU, TEA, DMF, RT; (c) iodobenzene diacetate, ethyl acetate/acetonitrile/water, 0 °C to RT; (d) cyclobutane carboxylic acid, HATU, TEA, DMF, RT; and (e) appropriate amine, phenyl chloroformate, TEA, tetrahydrofuran (THF), 0 °C to RT.



https://doi.org/10.1021/acs.jmedchem.0c02093
J. Med. Chem. 2021, 64, 3956−3975

fusion or *MET* amplification. In contrast, **13c** had almost no influence on cell proliferation in cell lines without *AXL* or *MET* aberration, even at high concentrations, confirming the selectivity of **13c** against Axl and Met. Compound **13c** also restrained Gas6/Axl-mediated cancer cell migration or invasion. Furthermore, **13c** exhibited significant antitumor activity in vivo in Axl-driven or Met-driven tumor xenografts, causing tumor stasis or regression at well-tolerant doses. Compound **13c** may serve as a potential Axl/Met dual inhibitor for further drug development.

## EXPERIMENTAL SECTION

**Chemistry.** Unless otherwise noted, all starting materials, reagents, and solvents were commercially available and used without further purification. Chemical reactions were monitored by thin-layer chromatography (TLC) or liquid chromatography (LC)/mass spectrometry (MS). TLC was performed using silica gel plates with fluorescence F254 and UV light visualization. LC/MS was performed on an Agilent 1200 HPLC/6110 MSD system (column: ZORBAX Eclipse Plus column, C18, 4.6 mm × 100 mm, 3.5 μm). Column chromatography was performed by automated flash chromatography on a Biotage Isolera One instrument using silica gel (300−400 mesh). $^1$H NMR and $^{13}$C NMR spectra were obtained using $CDCl_3$, DMSO-$d_6$, $CD_3OD$, or acetone-$d_6$ on Varian Mercury Plus 300 M or 400 M or Bruker AVANCE III 400 M, 500 M, or 600 M NMR spectrometers. In the tabulated NMR results, multiplicities are indicated by s (singlet), br s (broad singlet), d (doublet), dd (doublet of doublet), ddd (doublet of doublet of doublet), t (triplet), dt (doublet of triplets), q (quartet), p (pentet), and m (multiplet). High-resolution ESI-MS was performed on an Agilent G6520 Q-TOF spectrometer. The purity of all the final compounds was confirmed to be >95% as determined by HPLC on an Agilent infinity 1260 HPLC system (column: ZORBAX Eclipse Plus column, C18, 4.6 mm × 150 mm, 5 μm; detector: diode array detector). The mobile phase of methanol and water was used with a flow rate of 1.0 mL/min.

*1,5-Dimethyl-N-(4-((3-(1-methyl-1H-pyrazol-4-yl)pyridin-4-yl)-oxy)phenyl)-3-oxo-2-phenyl-2,3-dihydro-1H-pyrazole-4-carboxamide (**9**).* The compound was prepared from **16** and **17a** by following a similar procedure as described for **13c**. Light yellow solid, 86% yield. $^1$H NMR (300 MHz, DMSO-$d_6$): δ 10.82 (s, 1H), 8.86 (s, 1H), 8.29−8.19 (m, 2H), 8.03 (d, *J* = 0.8 Hz, 1H), 7.74−7.66 (m, 2H), 7.63−7.48 (m, 3H), 7.48−7.38 (m, 2H), 7.21−7.11 (m, 2H), 6.73−6.64 (m, 1H), 3.89 (s, 3H), 3.36 (s, 3H), 2.71 (s, 3H). $^{13}$C NMR (126 MHz, $CDCl_3$): δ 164.03, 161.69, 161.00, 155.14, 149.41, 148.78, 148.47, 137.71, 136.42, 133.17, 129.91, 129.87 (s, 2C), 129.15, 126.60 (s, 2C), 121.59 (s, 2C), 121.33 (s, 2C), 118.95, 114.89, 110.76, 99.78, 39.16, 33.60, 12.02. HRMS: $(M + H)^+$ calcd for $C_{27}H_{25}N_6O_3$, 481.1983; found, 481.1989.

*4-Ethoxy-1-(4-fluorophenyl)-N-(4-((3-(1-methyl-1H-pyrazol-4-yl)pyridin-4-yl)oxy)phenyl)-1H-pyrazole-3-carboxamide (**10a**).* The compound was prepared from **16** and **17b** by following a similar procedure as described for **13c**. Light yellow solid, 88% yield. $^1$H NMR (400 MHz, DMSO-$d_6$): δ 9.99 (s, 1H), 8.87 (s, 1H), 8.50 (s, 1H), 8.26 (d, *J* = 5.8 Hz, 2H), 8.07−7.98 (m, 3H), 7.94−7.86 (m, 2H), 7.42 (t, *J* = 8.8 Hz, 2H), 7.24−7.19 (m, 2H), 6.71 (d, *J* = 5.6 Hz, 1H), 4.11 (q, *J* = 7.0 Hz, 2H), 3.90 (s, 3H), 1.40 (t, *J* = 7.0 Hz, 3H). $^{13}$C NMR (126 MHz, $CDCl_3$): δ 161.74 (d, *J* = 247.5 Hz, 1C), 160.80, 159.05, 150.21, 149.10, 148.66, 146.42, 137.89, 136.16 (d, *J* = 2.8 Hz, 1C), 135.60, 134.93, 129.87, 121.73 (s, 2C), 121.49 (s, 2C), 121.17 (d, *J* = 8.4 Hz, 2C), 119.13, 116.52 (d, *J* = 23.2 Hz, 2C), 114.98, 112.82, 110.95, 68.85, 39.25, 14.99. HRMS: $(M + H)^+$ calcd for $C_{27}H_{24}FN_6O_3$, 499.1888; found, 499.1886.

*1-(4-Fluorophenyl)-2-methyl-N-(4-((3-(1-methyl-1H-pyrazol-4-yl)pyridin-4-yl)oxy)phenyl)-6-oxo-1,6-dihydropyrimidine-5-carboxamide (**10b**).* The compound was prepared from **16** and **17c** by following a similar procedure as described for **13c**. Light yellow solid, 50% yield. $^1$H NMR (300 MHz, DMSO-$d_6$): δ 11.17 (s, 1H), 8.86 (s, 1H), 8.82 (s, 1H), 8.30−8.22 (m, 2H), 8.02 (d, *J* = 0.8 Hz, 1H), 7.80 (d, *J* = 8.9 Hz, 2H), 7.61 (dd, *J* = 8.9, 5.1 Hz, 2H), 7.47 (t, *J* = 8.7 Hz, 2H), 7.19 (d, *J* = 8.9 Hz, 2H), 6.70 (d, *J* = 5.6 Hz, 1H), 3.88 (s, 3H), 2.23 (s, 3H). $^{13}$C NMR (126 MHz, $CDCl_3$): δ 163.37, 163.31 (d, *J* = 251.7 Hz, 1C), 162.81, 160.74, 160.60, 158.47, 150.36, 148.96, 148.51, 137.83, 135.51, 132.23 (d, *J* = 3.4 Hz), 129.83, 129.05 (d, *J* = 8.7 Hz, 2C), 122.17 (s, 2C), 121.36 (s, 2C), 119.15, 117.88 (d, *J* = 23.1 Hz, 2C), 115.89, 114.86, 110.97, 39.18, 24.73. HRMS: $(M + H)^+$ calcd for $C_{27}H_{22}FN_6O_3$, 497.1732; found, 497.1732.

*1-(4-Fluorophenyl)-2,4-dimethyl-N-(4-((3-(1-methyl-1H-pyrazol-4-yl)pyridin-4-yl)oxy)phenyl)-6-oxo-1,6-dihydropyrimidine-5-carboxamide (**10c**).* The compound was prepared from **16** and **17d** by following a similar procedure as described for **13c**. Light yellow solid, 69% yield. $^1$H NMR (300 MHz, DMSO-$d_6$): δ 10.73 (s, 1H), 8.85 (s, 1H), 8.23 (d, *J* = 5.6 Hz, 2H), 8.02 (s, 1H), 7.77 (d, *J* = 8.6 Hz, 2H), 7.44 (q, *J* = 8.8, 7.1 Hz, 4H), 7.17 (d, *J* = 8.6 Hz, 2H), 6.68 (d, *J* = 5.7 Hz, 1H), 3.89 (s, 3H), 2.41 (s, 3H), 2.14 (s, 3H). $^{13}$C NMR (151 MHz, $CDCl_3$): δ 171.26, 163.37, 163.16 (d, *J* = 251.5 Hz, 1C), 162.51, 160.84, 159.02, 149.99, 148.87, 148.47, 137.77, 135.88, 132.50 (d, *J* = 3.5 Hz, 1C), 129.84, 129.13 (d, *J* = 8.8 Hz, 2C), 122.35 (s, 2C), 121.28 (s, 2C), 119.01, 117.72 (d, *J* = 23.2 Hz, 2C), 114.85, 113.51, 110.82, 39.17, 26.11, 24.31. HRMS: $(M + H)^+$ calcd for $C_{28}H_{24}FN_6O_3$, 511.1888; found, 511.1886.

*3-(4-Fluorophenyl)-N-(4-((3-(1-methyl-1H-pyrazol-4-yl)pyridin-4-yl)oxy)phenyl)-2,4-dioxo-1,2,3,4-tetrahydropyrimidine-5-carboxamide (**10d**).* The compound was prepared from **16** and **17e** by following a similar procedure as described for **13c**. Light yellow solid, 69% yield. $^1$H NMR (300 MHz, DMSO-$d_6$): δ 12.37 (s, 1H), 10.86 (s, 1H), 8.84 (s, 1H), 8.41 (s, 1H), 8.26−8.20 (m, 2H), 8.03−7.99 (m, 1H), 7.78−7.72 (m, 2H), 7.45−7.29 (m, 4H), 7.19−7.11 (m, 2H), 6.67 (d, *J* = 5.7 Hz, 1H), 3.86 (s, 3H). $^{13}$C NMR (126 MHz, DMSO-$d_6$): δ 163.79, 161.77 (d, *J* = 245.0 Hz, 1C), 160.17, 159.59, 150.32, 149.59, 148.87, 148.42, 147.68, 137.33, 135.31, 131.00 (d, *J* = 3.0 Hz, 1C), 130.91 (d, *J* = 9.0 Hz, 2C), 130.09, 121.47 (s, 2C), 121.02 (s, 2C), 118.76, 115.87 (d, *J* = 22.9 Hz, 2C), 113.83, 110.84, 104.19, 38.60. HRMS: $(M + H)^+$ calcd for $C_{26}H_{20}FN_6O_4$, 499.1525; found, 499.1519.

*3-(4-Fluorophenyl)-1-methyl-N-(4-((3-(1-methyl-1H-pyrazol-4-yl)pyridin-4-yl)oxy)phenyl)-2,4-dioxo-1,2,3,4-tetrahydropyrimidine-5-carboxamide (**10e**).* The compound was prepared from **16** and **17f** by following a similar procedure as described for **13c**. Light brown solid, 47% yield. $^1$H NMR (300 MHz, DMSO-$d_6$): δ 10.90 (s, 1H), 8.85 (s, 2H), 8.25 (d, *J* = 2.8 Hz, 2H), 8.04−7.98 (m, 1H), 7.77 (dd, *J* = 8.9, 2.0 Hz, 2H), 7.46−7.30 (m, 4H), 7.22−7.12 (m, 2H), 6.70 (dd, *J* = 5.6, 2.0 Hz, 1H), 3.88 (s, 3H), 3.53 (s, 3H). $^{13}$C NMR (126 MHz, $CDCl_3$): δ 163.56, 162.95 (d, *J* = 249.6 Hz, 1C), 160.68, 159.84, 150.70 (s, 2C), 150.50, 149.11, 148.62, 137.90, 135.32, 130.08 (d, *J* = 3.3 Hz, 1C), 130.00 (d, *J* = 8.8 Hz, 2C), 129.80, 122.19 (s, 2C), 121.41 (s, 2C), 119.19, 117.02 (d, *J* = 22.9 Hz, 2C), 114.93, 111.02, 105.59, 39.23, 38.31. HRMS: $(M + H)^+$ calcd for $C_{27}H_{22}FN_6O_4$, 513.1681; found, 513.1686.

*1-Ethyl-3-(4-fluorophenyl)-N-(4-((3-(1-methyl-1H-pyrazol-4-yl)-pyridin-4-yl)oxy)phenyl)-2,4-dioxo-1,2,3,4-tetrahydropyrimidine-5-carboxamide (**10f**).* The compound was prepared from **16** and **17g** by following a similar procedure as described for **13c**. Light yellow solid, 72% yield. $^1$H NMR (300 MHz, DMSO-$d_6$): δ 10.90 (s, 1H), 8.86 (s, 2H), 8.26−8.22 (m, 2H), 8.04−7.99 (m, 1H), 7.82−7.73 (m, 2H), 7.48−7.30 (m, 4H), 7.18 (d, *J* = 8.9 Hz, 2H), 6.70 (d, *J* = 5.7 Hz, 1H), 4.01 (q, *J* = 6.9 Hz, 2H), 3.88 (s, 3H), 1.29 (t, *J* = 7.1 Hz, 3H). $^{13}$C NMR (126 MHz, $CDCl_3$): δ 163.48, 162.87 (d, *J* = 249.6 Hz, 1C), 160.75, 159.95, 150.39, 150.26, 149.69, 148.93, 148.45, 137.87, 135.36, 130.13 (d, *J* = 3.3 Hz, 1C), 130.02 (d, *J* = 8.7 Hz, 2C), 129.79, 122.16 (s, 2C), 121.39 (s, 2C), 119.20, 116.93 (d, *J* = 23.1 Hz, 2C), 114.84, 110.99, 105.70, 46.58, 39.19, 14.51. HRMS: $(M + H)^+$ calcd for $C_{28}H_{24}FN_6O_4$, 527.1838; found, 527.1837.

*3-(4-Fluorophenyl)-1-isopropyl-N-(4-((3-(1-methyl-1H-pyrazol-4-yl)pyridin-4-yl)oxy)phenyl)-2,4-dioxo-1,2,3,4-tetrahydropyrimidine-5-carboxamide (**10g**).* The compound was prepared from **16** and **17h** by following a similar procedure as described for **13c**. White solid, 75% yield. $^1$H NMR (300 MHz, DMSO-$d_6$): δ 10.90 (s, 1H), 8.84 (s, 1H), 8.64 (s, 1H), 8.25−8.20 (m, 2H), 8.01 (d, *J* = 0.8 Hz, 1H), 7.76 (d, *J* = 9.0 Hz, 2H), 7.47−7.29 (m, 4H), 7.16 (d, *J* = 8.9 Hz, 2H), 6.69 (d, *J* = 5.6 Hz, 1H), 4.76 (p, *J* = 6.7 Hz, 1H), 3.86 (s, 3H), 1.40 (d, *J* = 6.7 Hz, 6H). $^{13}$C NMR (126 MHz, $CDCl_3$): δ 163.07, 162.82 (d, *J* = 249.2 Hz, 1C), 160.64, 160.02, 150.44, 150.38, 149.06, 148.58, 146.28, 137.84,


https://doi.org/10.1021/acs.jmedchem.0c02093
J. Med. Chem. 2021, 64, 3956−3975

135.39, 130.32 (d, $J$ = 3.0 Hz, 1C), 130.00 (d, $J$ = 8.9 Hz, 2C), 129.76, 122.06 (s, 2C), 121.35 (s, 2C), 119.13, 116.89 (d, $J$ = 23.1 Hz, 2C), 114.87, 110.96, 105.74, 50.52, 39.17, 21.64 (s, 2C). HRMS: $(M + H)^+$ calcd for $C_{29}H_{26}FN_6O_4$, 541.1994; found, 542.0000.

*3-(4-Fluorophenyl)-N-(4-((3-(1-methyl-1H-pyrazol-4-yl)pyridin-4-yl)oxy)phenyl)-2,4-dioxo-1-((tetrahydro-2H-pyran-4-yl)methyl)-1,2,3,4-tetrahydropyrimidine-5-carboxamide (**10h**).* The compound was prepared from **16** and **17i** by following a similar procedure as described for **13c**. White solid, 71% yield. $^1$H NMR (300 MHz, DMSO-$d_6$): $\delta$ 10.93 (s, 1H), 8.86 (s, 1H), 8.80 (s, 1H), 8.28−8.22 (m, 2H), 8.02 (d, $J$ = 0.8 Hz, 1H), 7.77 (d, $J$ = 9.0 Hz, 2H), 7.47−7.32 (m, 4H), 7.18 (d, $J$ = 9.0 Hz, 2H), 6.70 (d, $J$ = 5.7 Hz, 1H), 3.95−3.81 (m, 7H), 3.26 (t, $J$ = 11.4 Hz, 2H), 1.99 (s, 1H), 1.59 (d, $J$ = 11.8 Hz, 2H), 1.35−1.20 (m, 2H). $^{13}$C NMR (126 MHz, $CDCl_3$): $\delta$ 163.34, 162.93 (d, $J$ = 249.8 Hz, 1C), 160.72, 159.79, 150.64, 150.52, 150.16, 149.12, 148.61, 137.93, 135.30, 130.08−129.92 (m, 3C), 129.78, 122.18 (s, 2C), 121.42 (s, 2C), 119.25, 117.00 (d, $J$ = 23.1 Hz, 2C), 114.88, 111.04, 105.51, 67.29 (s, 2C), 56.69, 39.24, 34.98, 30.35 (s, 2C). HRMS: $(M + H)^+$ calcd for $C_{32}H_{30}FN_6O_5$, 597.2256; found, 597.2262.

*4-(4-Fluorophenyl)-2-isopropyl-N-(4-((3-(1-methyl-1H-pyrazol-4-yl)pyridin-4-yl)oxy)phenyl)-3,5-dioxo-2,3,4,5-tetrahydro-1,2,4-triazine-6-carboxamide (**10i**).* The compound was prepared from **16** and **17j** by following a similar procedure as described for **13c**. Yellow solid, 60% yield. $^1$H NMR (400 MHz, DMSO-$d_6$): $\delta$ 10.70 (s, 1H), 8.85 (s, 1H), 8.27−8.20 (m, 2H), 8.01 (s, 1H), 7.83−7.73 (m, 2H), 7.47−7.32 (m, 4H), 7.20 (d, $J$ = 9.0 Hz, 2H), 6.70 (d, $J$ = 5.6 Hz, 1H), 4.88 (p, $J$ = 6.6 Hz, 1H), 3.87 (s, 3H), 1.36 (d, $J$ = 6.6 Hz, 6H). $^{13}$C NMR (126 MHz, $CDCl_3$): $\delta$ 163.16 (d, $J$ = 250.7 Hz, 1C), 160.53, 156.85, 156.63, 150.94, 149.12, 148.60, 147.59, 137.89, 134.88, 132.50, 129.77, 129.66 (d, $J$ = 8.9 Hz, 2C), 128.26 (d, $J$ = 3.4 Hz, 1 C), 122.22 (s, 2C), 121.40 (s, 2C), 119.24, 117.13 (d, $J$ = 23.2 Hz, 2C), 114.85, 111.10, 54.01, 39.20, 20.81 (s, 2C). HRMS: $(M + H)^+$ calcd for $C_{28}H_{25}FN_7O_4$, 542.1947; found, 542.1951.

*N-(4-((3-(1-Methyl-1H-pyrazol-4-yl)pyridin-4-yl)oxy)phenyl)-1-oxo-3-phenyl-1H-indene-2-carboxamide (**10j**).* The compound was prepared from **16** and **17k** by following a similar procedure as described for **13c**. Red solid, 36% yield. $^1$H NMR (300 MHz, DMSO-$d_6$): $\delta$ 10.44 (s, 1H), 8.86 (s, 1H), 8.27−8.22 (m, 2H), 8.02 (s, 1H), 7.73−7.47 (m, 10H), 7.38 (d, $J$ = 7.2 Hz, 1H), 7.21−7.13 (m, 2H), 6.68 (d, $J$ = 5.6 Hz, 1H), 3.89 (s, 3H). $^{13}$C NMR (126 MHz, $CDCl_3$): $\delta$ 197.19, 169.87, 160.70, 159.27, 150.11, 148.90, 148.46, 143.92, 137.73, 135.51, 134.56, 131.58, 131.48, 130.64, 130.28, 129.74, 128.50 (s, 2C), 128.11 (s, 2C), 124.26, 123.79, 122.11 (s, 2C), 122.07, 121.24 (s, 2C), 118.95, 114.82, 110.74, 39.11. HRMS: $(M + H)^+$ calcd for $C_{31}H_{23}N_4O_3$, 499.1765; found, 499.1764.

*N-(4-((3-(1-Methyl-1H-pyrazol-4-yl)pyridin-4-yl)oxy)phenyl)-3,8-dioxo-2-phenyl-2,3,5,6,7,8-hexahydroisoquinoline-4-carboxamide (**10k**).* The compound was prepared from **16** and **17l** by following a similar procedure as described for **13c**. Light brown solid, 58% yield. $^1$H NMR (300 MHz, $CDCl_3$): $\delta$ 11.29 (s, 1H), 8.77 (s, 1H), 8.50 (s, 1H), 8.24 (d, $J$ = 5.5 Hz, 1H), 7.93 (d, $J$ = 13.7 Hz, 2H), 7.72 (d, $J$ = 8.9 Hz, 2H), 7.63−7.50 (m, 3H), 7.38 (dd, $J$ = 7.8, 1.8 Hz, 2H), 7.07 (d, $J$ = 8.9 Hz, 2H), 6.65 (d, $J$ = 5.7 Hz, 1H), 3.95 (s, 3H), 3.63 (t, $J$ = 6.2 Hz, 2H), 2.65 (t, $J$ = 6.4 Hz, 2H), 2.12 (p, $J$ = 6.3 Hz, 2H). $^{13}$C NMR (126 MHz, $CDCl_3$): $\delta$ 195.03, 162.96, 162.33, 161.47, 160.94, 150.20, 148.99, 148.56, 143.24, 139.58, 137.89, 135.81, 130.04, 129.99 (s, 2C), 129.87, 126.40 (s, 2C), 122.51 (s, 2C), 121.36 (s, 2C), 119.17, 118.53, 116.59, 114.90, 110.95, 39.24, 38.18, 29.72, 21.68. HRMS: $(M + H)^+$ calcd for $C_{31}H_{26}N_5O_4$, 532.1979; found, 532.1979.

*1-(4-Fluorophenyl)-N-(4-((3-(1-methyl-1H-pyrazol-4-yl)pyridin-4-yl)oxy)phenyl)-2,5-dioxo-1,2,5,6,7,8-hexahydroquinoline-3-carboxamide (**10l**).* The compound was prepared from **16** and **17m** by following a similar procedure as described for **13c**. Light yellow solid, 23% yield. $^1$H NMR (300 MHz, $CDCl_3$): $\delta$ 11.38 (s, 1H), 9.33 (s, 1H), 8.78 (d, $J$ = 1.6 Hz, 1H), 8.25 (d, $J$ = 5.8 Hz, 1H), 7.93 (d, $J$ = 14.8 Hz, 2H), 7.77 (d, $J$ = 9.1 Hz, 2H), 7.40−7.28 (m, 4H), 7.07 (d, $J$ = 8.6 Hz, 2H), 6.65 (d, $J$ = 5.7 Hz, 1H), 3.96 (d, $J$ = 1.7 Hz, 3H), 2.67−2.53 (m, 4H), 2.19−2.07 (m, 2H). $^{13}$C NMR (126 MHz, $CDCl_3$): $\delta$ 192.86, 163.56, 163.18 (d, $J$ = 251.6 Hz, s, 1C), 160.77, 160.71, 159.71, 150.21, 148.90, 148.48, 142.09, 137.78, 135.67, 132.71 (d, $J$ = 3.2 Hz, 1C), 129.86, 129.43 (d, $J$ = 8.9 Hz, 2C), 122.16 (s, 2C), 121.32 (s, 2C), 119.96, 119.11, 117.77 (d, $J$ = 23.1 Hz, 2C), 115.78, 114.85, 110.92, 39.18, 36.51, 29.44, 21.15. HRMS: $(M + H)^+$ calcd for $C_{31}H_{25}FN_5O_4$, 550.1885; found, 550.1881.

*1-(4-Fluorophenyl)-N-(4-((3-(1-methyl-1H-pyrazol-4-yl)pyridin-4-yl)oxy)phenyl)-2-oxo-1,2-dihydro-1,7-naphthyridine-3-carboxamide (**10m**).* The compound was prepared from **16** and **17n** by following a similar procedure as described for **13c**. Yellow solid, 80% yield. $^1$H NMR (300 MHz, DMSO-$d_6$): $\delta$ 11.78 (s, 1H), 9.13 (s, 1H), 8.87 (s, 1H), 8.56 (d, $J$ = 5.1 Hz, 1H), 8.30−8.23 (m, 2H), 8.10 (d, $J$ = 4.7 Hz, 1H), 8.07−8.01 (m, 2H), 7.87 (d, $J$ = 9.0 Hz, 2H), 7.65−7.51 (m, 4H), 7.22 (d, $J$ = 9.0 Hz, 2H), 6.72 (d, $J$ = 5.7 Hz, 1H), 3.89 (s, 3H). $^{13}$C NMR (151 MHz, $CDCl_3$): $\delta$ 163.31 (d, $J$ = 251.3 Hz, 1C), 162.11, 160.71, 159.94, 150.66, 149.07, 148.59, 143.87, 143.66, 139.07, 137.89, 136.34, 135.33, 131.34 (d, $J$ = 3.3 Hz, 1C), 130.34 (d, $J$ = 8.9 Hz, 2C), 129.82, 126.75, 123.94, 122.42 (s, 2C), 121.89, 121.42 (s, 2C), 119.23, 118.10 (d, $J$ = 23.2 Hz, 2C), 114.85, 111.05, 39.24. HRMS: $(M + H)^+$ calcd for $C_{30}H_{22}FN_6O_3$, 533.1732; found, 533.1729.

*6-Ethyl-1,2-dimethyl-N-(4-((3-(1-methyl-1H-pyrazol-4-yl)pyridin-4-yl)oxy)phenyl)-4-oxo-1,4-dihydroquinoline-3-carboxamide (**10n**).* The compound was prepared from **16** and **17o** by following a similar procedure as described for **13c**. Light yellow solid, 50% yield. $^1$H NMR (400 MHz, DMSO-$d_6$): $\delta$ 10.81 (s, 1H), 8.84 (s, 1H), 8.29−8.19 (m, 2H), 8.06 (d, $J$ = 2.2 Hz, 1H), 8.02 (s, 1H), 7.81 (dd, $J$ = 9.0, 3.8 Hz, 3H), 7.65 (dd, $J$ = 8.9, 2.2 Hz, 1H), 7.17 (d, $J$ = 8.9 Hz, 2H), 6.68 (d, $J$ = 5.6 Hz, 1H), 3.89 (s, 3H), 3.82 (s, 3H), 2.75 (q, $J$ = 7.6 Hz, 2H), 2.62 (s, 3H), 1.23 (t, $J$ = 7.7 Hz, 3H). $^{13}$C NMR (126 MHz, $CDCl_3$): $\delta$ 176.55, 165.08, 161.00, 157.96, 149.60, 148.88, 148.55, 141.43, 138.71, 137.75, 136.83, 133.60, 129.94, 126.37, 125.28, 122.43 (s, 2C), 121.30 (s, 2C), 118.92, 115.89, 114.99, 113.98, 110.79, 39.19, 35.79, 28.36, 20.42, 15.42. HRMS: $(M + H)^+$ calcd for $C_{29}H_{28}N_5O_3$, 494.2187; found, 494.2189.

*3-(4-Fluorophenyl)-1-isopropyl-N-(4-((2-(1-methyl-1H-pyrazol-4-yl)pyridin-4-yl)oxy)phenyl)-2,4-dioxo-1,2,3,4-tetrahydropyrimidine-5-carboxamide (**11a**).* The compound was prepared from **20a** and **17h** by following a similar procedure as described for **13c**. White solid, 87% yield. $^1$H NMR (300 MHz, DMSO-$d_6$): $\delta$ 10.92 (s, 1H), 8.66 (s, 1H), 8.36 (d, $J$ = 5.7 Hz, 1H), 8.25 (s, 1H), 7.96 (d, $J$ = 0.8 Hz, 1H), 7.77 (d, $J$ = 9.0 Hz, 2H), 7.47−7.31 (m, 4H), 7.23 (d, $J$ = 2.3 Hz, 1H), 7.18 (d, $J$ = 9.0 Hz, 2H), 6.63 (dd, $J$ = 5.7, 2.4 Hz, 1H), 4.77 (p, $J$ = 6.9 Hz, 1H), 3.85 (s, 3H), 1.42 (d, $J$ = 6.8 Hz, 6H). $^{13}$C NMR (126 MHz, $CDCl_3$): $\delta$ 165.62, 163.09, 162.87 (d, $J$ = 249.5 Hz, 1C), 160.06, 153.95, 151.19, 150.50, 150.44, 146.30, 137.66, 135.35, 130.35 (d, $J$ = 3.5 Hz, 1C), 130.03 (d, $J$ = 8.8 Hz, 2C), 129.16, 123.38, 122.01 (s, 2C), 121.45 (s, 2C), 116.94 (d, $J$ = 23.1 Hz, 2C), 109.78, 107.68, 105.80, 50.55, 39.26, 21.68 (s, 2C). HRMS: $(M + H)^+$ calcd for $C_{29}H_{26}FN_6O_4$, 541.1994; found, 541.1993.

*N-(3-Fluoro-4-((2-(1-methyl-1H-pyrazol-4-yl)pyridin-4-yl)oxy)-phenyl)-3-(4-fluorophenyl)-1-isopropyl-2,4-dioxo-1,2,3,4-tetrahydropyrimidine-5-carboxamide (**11b**).* The compound was prepared from **20b** and **17h** by following a similar procedure as described for **13c**. White solid, 95% yield. $^1$H NMR (300 MHz, $CDCl_3$): $\delta$ 10.93 (s, 1H), 8.68 (s, 1H), 8.37 (dd, $J$ = 5.7, 0.6 Hz, 1H), 7.92−7.80 (m, 3H), 7.31−7.22 (m, 5H), 7.12 (t, $J$ = 8.6 Hz, 1H), 6.97 (d, $J$ = 2.4 Hz, 1H), 6.61 (dd, $J$ = 5.8, 2.4 Hz, 1H), 4.95 (p, $J$ = 6.8 Hz, 1H), 3.92 (s, 3H), 1.49 (d, $J$ = 6.8 Hz, 6H). $^{13}$C NMR (126 MHz, $CDCl_3$): $\delta$ 165.13, 163.10, 162.89 (d, $J$ = 249.5 Hz, 1C), 160.21, 154.44 (d, $J$ = 249.3 Hz, 1C), 154.05, 151.27, 150.42, 146.52, 137.68, 137.04 (d, $J$ = 12.5 Hz, 1C), 136.62 (d, $J$ = 9.6 Hz, 1C), 130.26 (d, $J$ = 3.3 Hz, 1C), 130.00 (d, $J$ = 8.9 Hz, 2C), 129.18, 123.64, 123.40, 116.97 (d, $J$ = 23.2 Hz, 2C), 116.39 (d, $J$ = 3.6 Hz, 1C), 109.77 (d, $J$ = 23.3 Hz, 1C), 108.75, 106.83, 105.50, 50.65, 39.26, 21.69 (s, 2C). HRMS: $(M + H)^+$ calcd for $C_{29}H_{25}F_2N_6O_4$, 559.1900; found, 559.1902.

*N-(2-Fluoro-4-((2-(1-methyl-1H-pyrazol-4-yl)pyridin-4-yl)oxy)-phenyl)-3-(4-fluorophenyl)-1-isopropyl-2,4-dioxo-1,2,3,4-tetrahydropyrimidine-5-carboxamide (**11c**).* The compound was prepared from **20c** and **17h** by following a similar procedure as described for **13c**. White solid, 76% yield. $^1$H NMR (400 MHz, DMSO-$d_6$): $\delta$ 11.16 (s, 1H), 8.69 (s, 1H), 8.45 (t, $J$ = 9.1 Hz, 1H), 8.38 (d, $J$ = 5.5 Hz, 1H), 8.26 (s, 1H), 7.97 (s, 1H), 7.48−7.24 (m, 6H), 7.07 (d, $J$ = 9.1 Hz, 1H), 6.75−6.67 (m, 1H), 4.78 (p, $J$ = 6.5 Hz, 1H), 3.86 (s, 3H), 1.42 (d, $J$ = 6.6 Hz, 6H). $^{13}$C NMR (126 MHz, $CDCl_3$): $\delta$ 165.01, 162.85 (d, $J$ =


https://doi.org/10.1021/acs.jmedchem.0c02093
J. Med. Chem. 2021, 64, 3956−3975

249.4 Hz, 1C), 162.83, 160.31, 154.16, 153.44 (d, $J$ = 248.8 Hz, 1C), 151.34, 150.53, 150.45, 146.37, 137.66, 130.29 (d, $J$ = 3.3 Hz, 1C), 130.08 (d, $J$ = 8.9 Hz, 2C), 129.20, 123.91 (d, $J$ = 10.4 Hz, 1C), 123.29–123.18 (m, 2C), 116.89 (d, $J$ = 23.0 Hz, 2C), 116.48 (d, $J$ = 3.6 Hz, 1C), 109.93, 108.47 (d, $J$ = 21.8 Hz, 1C), 107.90, 105.73, 50.55, 39.26, 21.67 (s, 2C). HRMS: $(M - H)^-$ calcd for $C_{29}H_{23}F_2N_6O_4$, 557.1754; found, 557.1757.

*N-(3-Chloro-4-((2-(1-methyl-1H-pyrazol-4-yl)pyridin-4-yl)oxy)-phenyl)-3-(4-fluorophenyl)-1-isopropyl-2,4-dioxo-1,2,3,4-tetrahydropyrimidine-5-carboxamide (**11d**).* The compound was prepared from **20d** and **17h** by following a similar procedure as described for **13c**. White solid, 59% yield. $^1$H NMR (400 MHz, acetone-$d_6$): $\delta$ 11.05 (s, 1H), 8.66 (s, 1H), 8.37 (d, $J$ = 5.7 Hz, 1H), 8.23 (d, $J$ = 2.5 Hz, 1H), 8.11 (s, 1H), 7.93 (d, $J$ = 0.8 Hz, 1H), 7.66 (dd, $J$ = 8.8, 2.6 Hz, 1H), 7.50–7.40 (m, 2H), 7.39–7.26 (m, 3H), 7.14 (d, $J$ = 2.4 Hz, 1H), 6.59 (dd, $J$ = 5.7, 2.4 Hz, 1H), 4.93 (p, $J$ = 6.8 Hz, 1H), 3.90 (s, 3H), 1.50 (d, $J$ = 6.8 Hz, 6H). $^{13}$C NMR (126 MHz, $CDCl_3$): $\delta$ 164.88, 163.13, 162.93 (d, $J$ = 249.7 Hz, 1C), 160.25, 154.10, 151.31, 150.44, 146.54, 145.89, 137.72, 136.46, 130.26 (d, $J$ = 3.7 Hz, 1C), 130.02 (d, $J$ = 8.8 Hz, 2C), 129.20, 127.65, 123.44, 123.38, 122.63, 119.96, 117.00 (d, $J$ = 23.3 Hz, 2C), 109.00, 107.08, 105.53, 50.67, 39.29, 21.73 (s, 2C). HRMS: $(M + H)^+$ calcd for $C_{29}H_{25}ClFN_6O_4$, 575.1604; found, 575.1603.

*3-(4-Fluorophenyl)-1-isopropyl-N-(3-methyl-4-((2-(1-methyl-1H-pyrazol-4-yl)pyridin-4-yl)oxy)phenyl)-2,4-dioxo-1,2,3,4-tetrahydropyrimidine-5-carboxamide (**11e**).* The compound was prepared from **20e** and **17h** by following a similar procedure as described for **13c**. White solid, 70% yield. $^1$H NMR (400 MHz, DMSO-$d_6$): $\delta$ 10.91 (s, 1H), 8.66 (s, 1H), 8.33 (d, $J$ = 5.8 Hz, 1H), 8.24 (s, 1H), 7.95 (s, 1H), 7.71–7.62 (m, 2H), 7.47–7.32 (m, 4H), 7.18 (d, $J$ = 2.5 Hz, 1H), 7.09 (d, $J$ = 8.4 Hz, 1H), 6.51 (dd, $J$ = 5.7, 2.4 Hz, 1H), 4.78 (p, $J$ = 6.8 Hz, 1H), 3.85 (s, 3H), 2.10 (s, 3H), 1.42 (d, $J$ = 6.8 Hz, 6H). $^{13}$C NMR (126 MHz, $CDCl_3$): $\delta$ 165.53, 163.08, 162.86 (d, $J$ = 249.5 Hz, 1C), 160.03, 153.91, 151.17, 150.50, 148.34, 146.23, 137.66, 135.57, 131.54, 130.36 (d, $J$ = 3.4 Hz, 1C), 130.03 (d, $J$ = 8.9 Hz, 2C), 129.16, 123.48, 123.39, 121.96, 119.40, 116.93 (d, $J$ = 23.1 Hz, 2C), 108.97, 106.91, 105.86, 50.50, 39.25, 21.69 (s, 2C), 16.33. HRMS: $(M + H)^+$ calcd for $C_{30}H_{28}FN_6O_4$, 555.2151; found, 555.2155.

*3-(4-Fluorophenyl)-1-isopropyl-N-(3-methoxy-4-((2-(1-methyl-1H-pyrazol-4-yl)pyridin-4-yl)oxy)phenyl)-2,4-dioxo-1,2,3,4-tetrahydropyrimidine-5-carboxamide (**11f**).* The compound was prepared from **20f** and **17h** by following a similar procedure as described for **13c**. White solid, 72% yield. $^1$H NMR (400 MHz, acetone-$d_6$): $\delta$ 10.96 (s, 1H), 8.66 (s, 1H), 8.30 (d, $J$ = 5.7 Hz, 1H), 8.08 (s, 1H), 7.90 (s, 1H), 7.70 (d, $J$ = 2.4 Hz, 1H), 7.52–7.38 (m, 3H), 7.38–7.28 (m, 2H), 7.13 (d, $J$ = 8.6 Hz, 1H), 7.06 (d, $J$ = 2.4 Hz, 1H), 6.53 (dd, $J$ = 5.7, 2.4 Hz, 1H), 4.94 (p, $J$ = 6.8 Hz, 1H), 3.90 (s, 3H), 3.81 (s, 3H), 1.51 (d, $J$ = 6.8 Hz, 6H). $^{13}$C NMR (126 MHz, $CDCl_3$): $\delta$ 165.69, 163.14, 162.91 (d, $J$ = 249.5 Hz, 1C), 160.11, 153.75, 151.94, 151.03, 150.50, 146.27, 138.40, 137.68, 136.76, 130.35 (d, $J$ = 3.4 Hz, 1C), 130.03 (d, $J$ = 8.8 Hz, 2C), 129.10, 123.58, 122.99, 117.00 (d, $J$ = 23.2 Hz, 2C), 112.53, 108.79, 106.87, 105.79, 105.47, 56.02, 50.51, 39.26, 21.72 (s, 2C). HRMS: $(M + H)^+$ calcd for $C_{30}H_{28}FN_6O_5$, 571.2100; found, 571.2106.

*N-(2,3-Difluoro-4-((2-(1-methyl-1H-pyrazol-4-yl)pyridin-4-yl)-oxy)phenyl)-3-(4-fluorophenyl)-1-isopropyl-2,4-dioxo-1,2,3,4-tetrahydropyrimidine-5-carboxamide (**11g**).* The compound was prepared from **20g** and **17h** by following a similar procedure as described for **13c**. Off-white solid, 52% yield. $^1$H NMR (400 MHz, DMSO-$d_6$): $\delta$ 11.27 (s, 1H), 8.71 (s, 1H), 8.40 (d, $J$ = 5.7 Hz, 1H), 8.31–8.19 (m, 2H), 7.99 (s, 1H), 7.48–7.32 (m, 4H), 7.32–7.22 (m, 2H), 6.77 (dd, $J$ = 5.9, 2.4 Hz, 1H), 4.78 (p, $J$ = 6.9 Hz, 1H), 3.86 (s, 3H), 1.43 (d, $J$ = 6.7 Hz, 6H). $^{13}$C NMR (126 MHz, $CDCl_3$): $\delta$ 164.76, 162.88 (d, $J$ = 249.3 Hz, 1C), 162.85, 160.56, 154.21, 151.38, 150.46, 146.60, 144.25 (dd, $J$ = 99.4, 12.6 Hz, 1C), 142.25 (dd, $J$ = 97.9, 12.5 Hz, 1C), 138.13 (d, $J$ = 9.5 Hz 1C), 137.68, 130.19 (d, $J$ = 3.3 Hz, 1C), 130.06 (d, $J$ = 8.7 Hz, 2C), 129.25, 125.72 (d, $J$ = 8.0 Hz, 1C), 123.26, 117.57 (d, $J$ = 3.8 Hz, 2C), 116.93 (d, $J$ = 23.2 Hz, 1C), 116.64 (d, $J$ = 3.9 Hz, 1C), 108.85, 106.97, 105.45, 50.65, 39.26, 21.67 (s, 2C). HRMS: $(M - H)^-$ calcd for $C_{29}H_{22}F_3N_6O_4$, 575.1660; found, 575.1667.

*N-(2,5-Difluoro-4-((2-(1-methyl-1H-pyrazol-4-yl)pyridin-4-yl)-oxy)phenyl)-3-(4-fluorophenyl)-1-isopropyl-2,4-dioxo-1,2,3,4-tetrahydropyrimidine-5-carboxamide (**11h**).* The compound was prepared from **24** and **17h** by following a similar procedure as described for **13c**. Light brown solid, 56% yield. $^1$H NMR (400 MHz, DMSO-$d_6$): $\delta$ 11.34 (s, 1H), 8.72 (s, 1H), 8.48 (dd, $J$ = 12.5, 7.2 Hz, 1H), 8.39 (d, $J$ = 5.7 Hz, 1H), 8.28 (s, 1H), 7.99 (s, 1H), 7.61 (dd, $J$ = 11.1, 7.4 Hz, 1H), 7.47–7.33 (m, 4H), 7.27 (d, $J$ = 2.4 Hz, 1H), 6.74 (dd, $J$ = 5.7, 2.5 Hz, 1H), 4.78 (p, $J$ = 6.7 Hz, 1H), 3.86 (s, 3H), 1.43 (d, $J$ = 6.7 Hz, 6H). $^{13}$C NMR (126 MHz, $CDCl_3$): $\delta$ 164.66, 162.86 (d, $J$ = 249.4 Hz, 1C), 162.82, 160.40, 154.20, 151.36, 150.45, 149.56–147.46 (m, 2C), 146.61, 137.68, 136.10 (dd, $J$ = 14.3, 10.2 Hz, 1C), 130.19 (d, $J$ = 3.6 Hz, 1C), 130.05 (d, $J$ = 8.8 Hz, 2C), 129.23, 124.82 (t, $J$ = 11.2 Hz, 1C), 123.28, 116.91 (d, $J$ = 23.2 Hz, 2C), 110.58 (d, $J$ = 26.2 Hz, 1C), 110.17 (d, $J$ = 23.3 Hz, 1C), 108.76, 106.86, 105.40, 50.68, 39.26, 21.67 (s, 2C). HRMS: $(M + H)^+$ calcd for $C_{29}H_{24}F_3N_6O_4$, 577.1806; found, 577.1812.

*N-(3,5-Difluoro-4-((2-(1-methyl-1H-pyrazol-4-yl)pyridin-4-yl)-oxy)phenyl)-3-(4-fluorophenyl)-1-isopropyl-2,4-dioxo-1,2,3,4-tetrahydropyrimidine-5-carboxamide (**11i**).* The compound was prepared from **20h** and **17h** by following a similar procedure as described for **13c**. Off-white solid, 62% yield. $^1$H NMR (400 MHz, DMSO-$d_6$): $\delta$ 11.11 (s, 1H), 8.69 (s, 1H), 8.39 (d, $J$ = 5.7 Hz, 1H), 8.29 (s, 1H), 8.00 (d, $J$ = 0.7 Hz, 1H), 7.79 (d, $J$ = 10.3 Hz, 2H), 7.48–7.28 (m, 5H), 6.74 (dd, $J$ = 5.8, 2.5 Hz, 1H), 4.78 (p, $J$ = 6.8 Hz, 1H), 3.86 (s, 3H), 1.43 (d, $J$ = 6.8 Hz, 6H). $^{13}$C NMR (126 MHz, $CDCl_3$): $\delta$ 164.60, 163.07, 162.89 (d, $J$ = 249.7 Hz, 1C), 160.39, 155.70 (dd, $J$ = 249.7, 5.9 Hz, 2C), 154.13, 151.31, 150.34, 146.73, 137.69, 136.28 (t, $J$ = 12.3 Hz, 1C), 130.15 (d, $J$ = 3.5 Hz, 1C), 129.96 (d, $J$ = 8.7 Hz, 2C), 129.23, 125.69 (t, $J$ = 15.6 Hz, 1C), 123.29, 116.96 (d, $J$ = 23.2 Hz, 2C), 107.96, 106.23, 105.15, 104.73–104.45 (m, 2C), 50.74, 39.24, 21.65 (s, 2C). HRMS: $(M + H)^+$ calcd for $C_{29}H_{24}F_3N_6O_4$, 577.1806; found, 577.1809.

*N-(4-((2-(1,3-Dimethyl-1H-pyrazol-4-yl)pyridin-4-yl)oxy)-3-fluorophenyl)-3-(4-fluorophenyl)-1-isopropyl-2,4-dioxo-1,2,3,4-tetrahydropyrimidine-5-carboxamide (**12a**).* The compound was prepared from **20i** and **17h** by following a similar procedure as described for **13c**. Off-white solid, 97% yield. $^1$H NMR (400 MHz, DMSO-$d_6$): $\delta$ 11.01 (s, 1H), 8.66 (s, 1H), 8.39 (d, $J$ = 5.8 Hz, 1H), 8.12 (s, 1H), 7.97 (dd, $J$ = 12.9, 2.5 Hz, 1H), 7.53–7.30 (m, 6H), 7.04 (d, $J$ = 2.4 Hz, 1H), 6.67 (dd, $J$ = 5.7, 2.5 Hz, 1H), 4.76 (p, $J$ = 6.7 Hz, 1H), 3.75 (s, 3H), 2.35 (s, 3H), 1.41 (d, $J$ = 6.8 Hz, 6H). $^{13}$C NMR (126 MHz, $CDCl_3$): $\delta$ 164.88, 163.06, 162.84 (d, $J$ = 249.7 Hz, 1C), 160.15, 155.02, 154.41 (d, $J$ = 249.1 Hz, 1C), 151.12, 150.37, 146.66, 146.48, 137.00 (d, $J$ = 12.6 Hz, 1C), 136.58 (d, $J$ = 9.5 Hz, 1C), 130.87, 130.23 (d, $J$ = 3.3 Hz, 1C), 129.97 (d, $J$ = 8.7 Hz, 2C), 123.61, 120.54, 116.91 (d, $J$ = 23.1 Hz, 2C), 116.30 (d, $J$ = 3.4 Hz, 1C), 109.64 (d, $J$ = 23.3 Hz, 1 C), 108.17, 107.80, 105.44, 50.61, 38.80, 21.63 (s, 2C), 14.03. HRMS: $(M + H)^+$ calcd for $C_{30}H_{27}F_2N_6O_4$, 573.2056; found, 573.2062.

*N-(4-((2-(1-Cyclopropyl-1H-pyrazol-4-yl)pyridin-4-yl)oxy)-3-fluorophenyl)-3-(4-fluorophenyl)-1-isopropyl-2,4-dioxo-1,2,3,4-tetrahydropyrimidine-5-carboxamide (**12b**).* The compound was prepared from **20j** and **17h** by following a similar procedure as described for **13c**. Off-white solid, 73% yield. $^1$H NMR (400 MHz, $CDCl_3$): $\delta$ 10.94 (s, 1H), 8.69 (s, 1H), 8.38 (d, $J$ = 5.7 Hz, 1H), 7.97 (s, 1H), 7.89–7.81 (m, 2H), 7.26–7.23 (m, 5H), 7.13 (t, $J$ = 8.7 Hz, 1H), 6.97 (d, $J$ = 2.4 Hz, 1H), 6.62 (dd, $J$ = 6.0, 2.3 Hz, 1H), 4.97 (p, $J$ = 6.8 Hz, 1H), 3.70–3.57 (m, 1H), 1.50 (d, $J$ = 6.8 Hz, 6H), 1.19–1.12 (m, 2H), 1.07–1.00 (m, 2H). $^{13}$C NMR (126 MHz, $CDCl_3$): $\delta$ 165.13, 163.09, 162.89 (d, $J$ = 249.5 Hz, 1C), 160.20, 154.43 (d, $J$ = 249.1 Hz, 1C), 154.00, 151.26, 150.41, 146.52, 137.66, 137.04 (d, $J$ = 12.5 Hz, 1C), 136.62 (d, $J$ = 9.6 Hz, 1C), 130.25 (d, $J$ = 3.6 Hz, 1C), 130.00 (d, $J$ = 8.9 Hz, 2C), 128.62, 123.62, 122.85, 116.96 (d, $J$ = 23.2 Hz, 1C), 116.38 (d, $J$ = 3.4 Hz, 2C), 109.76 (d, $J$ = 23.3 Hz, 1C), 108.79, 106.86, 105.50, 50.65, 33.08, 21.69 (s, 2C), 6.66 (s, 2C). HRMS: $(M + H)^+$ calcd for $C_{31}H_{27}F_2N_6O_4$, 585.2056; found, 585.2060.

*N-(3-Fluoro-4-((2-(1-(2-hydroxy-2-methylpropyl)-1H-pyrazol-4-yl)pyridin-4-yl)oxy)phenyl)-3-(4-fluorophenyl)-1-isopropyl-2,4-dioxo-1,2,3,4-tetrahydropyrimidine-5-carboxamide (**12c**).* The compound was prepared from **20k** and **17h** by following a similar procedure as described for **13c**. Off-white solid, 89% yield. $^1$H NMR (400 MHz, DMSO-$d_6$): $\delta$ 11.03 (s, 1H), 8.68 (s, 1H), 8.37 (d, $J$ = 5.7 Hz, 1H), 8.22 (s, 1H), 8.05–7.92 (m, 2H), 7.59–7.20 (m, 7H), 6.65 (dd, $J$ = 5.8, 2.4 Hz, 1H), 4.78 (p, $J$ = 6.6 Hz, 1H), 4.72 (s, 1H), 4.03 (s, 2H), 1.42 (d, $J$ = 6.7 Hz, 6H), 1.07 (s, 6H). $^{13}$C NMR (126 MHz, $CDCl_3$): $\delta$ 165.19,


https://doi.org/10.1021/acs.jmedchem.0c02093
J. Med. Chem. 2021, 64, 3956–3975

163.09, 162.89 (d, $J$ = 249.6 Hz, 1C), 160.21, 154.42 (d, $J$ = 249.1 Hz, 1C), 153.79, 151.29, 150.41, 146.53, 138.08, 136.97 (d, $J$ = 12.5 Hz, 1C), 136.67 (d, $J$ = 9.9 Hz, 1C), 130.25 (d, $J$ = 3.6 Hz, 1C), 130.06 (d, $J$ = 5.1 Hz, 2C), 129.97, 123.64, 122.94, 116.96 (d, $J$ = 23.2 Hz, 2C), 116.40 (d, $J$ = 3.3 Hz, 1C), 109.78 (d, $J$ = 23.2 Hz, 1C), 108.90, 106.98, 105.48, 70.77, 62.28, 50.66, 26.96 (s, 2C), 21.68 (s, 2C). HRMS: $(M + H)^+$ calcd for $C_{32}H_{31}F_2N_6O_5$, 617.2319; found, 617.2325.

*N-(3-Fluoro-4-((2-(1-(2-(4-methylpiperazin-1-yl)ethyl)-1H-pyrazol-4-yl)pyridin-4-yl)oxy)phenyl)-3-(4-fluorophenyl)-1-isopropyl-2,4-dioxo-1,2,3,4-tetrahydropyrimidine-5-carboxamide (**12d**).* The compound was prepared from **20l** and **17h** by following a similar procedure as described for **13c**. Tan solid, 75% yield. $^1$H NMR (400 MHz, $CD_3OD$): $\delta$ 8.72 (s, 1H), 8.34 (d, $J$ = 5.8 Hz, 1H), 8.19 (s, 1H), 7.97 (s, 1H), 7.93 (dd, $J$ = 12.6, 2.5 Hz, 1H), 7.39−7.32 (m, 3H), 7.30−7.23 (m, 3H), 7.20 (d, $J$ = 2.5 Hz, 1H), 6.72 (dd, $J$ = 5.9, 2.5 Hz, 1H), 4.95−4.89 (m, 1H), 4.30 (t, $J$ = 6.0 Hz, 2H), 3.08−2.91 (m, 4H), 2.89 (t, $J$ = 6.0 Hz, 2H), 2.79−2.55 (m, 7H), 1.48 (d, $J$ = 6.8 Hz, 6H). $^{13}$C NMR (126 MHz, $CDCl_3$): $\delta$ 165.11, 162.96, 162.73 (d, $J$ = 249.4 Hz, 1C), 160.13, 154.22 (d, $J$ = 248.6 Hz, 1C), 153.66, 150.93, 150.30, 146.49, 137.55, 136.75 (d, $J$ = 12.6 Hz, 1C), 136.53 (d, $J$ = 9.6 Hz, 1C), 130.17 (d, $J$ = 3.2 Hz, 1C), 129.91 (d, $J$ = 8.8 Hz, 2C), 128.89, 123.52, 122.78, 116.80 (d, $J$ = 23.1 Hz, 2C), 116.32 (d, $J$ = 2.5 Hz, 1C), 109.61 (d, $J$ = 23.1 Hz, 1C), 108.66, 106.85, 105.29, 56.82, 54.04 (s, 2C), 50.71 (s, 2C), 50.59, 49.83, 44.21, 21.51 (s, 2C). HRMS: $(M + H)^+$ calcd for $C_{35}H_{37}F_2N_8O_4$, 671.2900; found, 671.2909.

*N-(4-((2-(1H-Pyrazol-4-yl)pyridin-4-yl)oxy)-3-fluorophenyl)-3-(4-fluorophenyl)-1-isopropyl-2,4-dioxo-1,2,3,4-tetrahydropyrimidine-5-carboxamide (**12e**).* The compound was prepared from **20m** and **17h** by following a similar procedure as described for **13c**. Light brown solid, 26% yield. $^1$H NMR (400 MHz, DMSO-$d_6$): $\delta$ 13.07 (s, 1H), 11.03 (s, 1H), 8.68 (s, 1H), 8.40−8.31 (m, 2H), 8.07−7.94 (m, 2H), 7.54−7.31 (m, 7H), 6.62 (dd, $J$ = 5.7, 2.5 Hz, 1H), 4.78 (p, $J$ = 6.8 Hz, 1H), 1.42 (d, $J$ = 6.8 Hz, 6H). $^{13}$C NMR (126 MHz, acetone-$d_6$): $\delta$ 165.98, 164.11, 163.33 (d, $J$ = 245.7 Hz, 1C), 161.39, 155.49, 155.03 (d, $J$ = 246.0 Hz, 1C), 152.11, 151.27, 147.80, 138.24 (d, $J$ = 9.9 Hz, 1C), 137.85, 137.31 (d, $J$ = 12.5 Hz, 1C), 132.66 (d, $J$ = 3.2 Hz, 1C), 131.69 (d, $J$ = 8.9 Hz, 2C), 125.81, 124.59, 123.40, 117.14 (d, $J$ = 3.3 Hz, 1C), 116.71 (d, $J$ = 23.2 Hz, 2C), 109.63 (d, $J$ = 23.6 Hz, 1C), 108.97, 107.40, 105.67, 51.53, 21.28 (s, 2C). HRMS: $(M + H)^+$ calcd for $C_{28}H_{23}F_2N_6O_4$, 545.1743; found, 545.1747.

*N-(4-((2-Acetamidopyridin-4-yl)oxy)-3-fluorophenyl)-3-(4-fluorophenyl)-1-isopropyl-2,4-dioxo-1,2,3,4-tetrahydropyrimidine-5-carboxamide (**13a**).* The compound was prepared from **28a** and **17h** by following a similar procedure as described for **13c**. Off-white solid, 40% yield. $^1$H NMR (400 MHz, DMSO-$d_6$): $\delta$ 11.03 (s, 1H), 10.58 (s, 1H), 8.68 (s, 1H), 8.18 (d, $J$ = 5.8 Hz, 1H), 7.98 (dd, $J$ = 12.9, 2.5 Hz, 1H), 7.65 (d, $J$ = 2.4 Hz, 1H), 7.56−7.31 (m, 6H), 6.68 (dd, $J$ = 5.7, 2.5 Hz, 1H), 4.77 (p, $J$ = 6.7 Hz, 1H), 2.03 (s, 3H), 1.42 (d, $J$ = 6.8 Hz, 6H). $^{13}$C NMR (126 MHz, $CDCl_3$): $\delta$ 168.86, 166.41, 163.07, 162.91 (d, $J$ = 249.8 Hz, 1C), 160.13, 154.39 (d, $J$ = 249.1 Hz, 1C), 153.31, 150.48, 149.04, 146.49, 137.04 (d, $J$ = 12.5 Hz, 1C), 136.71 (d, $J$ = 9.6 Hz, 1C), 130.30 (d, $J$ = 3.7 Hz, 1C), 130.04 (d, $J$ = 8.9 Hz, 2C), 123.64, 116.97 (d, $J$ = 23.1 Hz, 2C), 116.35 (d, $J$ = 3.4 Hz, 1C), 109.72 (d, $J$ = 23.4 Hz, 1C), 107.87, 105.60, 101.28, 50.66, 24.79, 21.71 (s, 2C). HRMS: $(M + H)^+$ calcd for $C_{27}H_{24}F_2N_5O_5$, 536.1740; found, 536.1742.

*N-(3-Fluoro-4-((2-propionamidopyridin-4-yl)oxy)phenyl)-3-(4-fluorophenyl)-1-isopropyl-2,4-dioxo-1,2,3,4-tetrahydropyrimidine-5-carboxamide (**13b**).* The compound was prepared from **28b** and **17h** by following a similar procedure as described for **13c**. Off-white solid, 30% yield. $^1$H NMR (400 MHz, DMSO-$d_6$): $\delta$ 11.03 (s, 1H), 10.51 (s, 1H), 8.68 (s, 1H), 8.18 (d, $J$ = 5.7 Hz, 1H), 7.98 (dd, $J$ = 12.9, 2.5 Hz, 1H), 7.66 (d, $J$ = 2.5 Hz, 1H), 7.55−7.30 (m, 6H), 6.70 (dd, $J$ = 5.8, 2.5 Hz, 1H), 4.78 (p, $J$ = 6.7 Hz, 1H), 2.34 (q, $J$ = 7.5 Hz, 2H), 1.42 (d, $J$ = 6.7 Hz, 6H), 1.00 (t, $J$ = 7.5 Hz, 3H). $^{13}$C NMR (126 MHz, $CDCl_3$): $\delta$ 172.56, 166.40, 163.07, 162.89 (d, $J$ = 249.6 Hz, 1C), 160.12, 154.38 (d, $J$ = 249.6 Hz, 1C), 153.37, 150.48, 149.01, 146.49, 137.03 (d, $J$ = 12.6 Hz, 1C), 136.68 (d, $J$ = 9.8 Hz, 1C), 130.30 (d, $J$ = 3.6 Hz, 1C), 130.04 (d, $J$ = 8.8 Hz, 2C), 123.63, 116.95 (d, $J$ = 23.1 Hz, 2C), 116.36 (d, $J$ = 3.3 Hz, 1C), 109.72 (d, $J$ = 23.3 Hz, 1C), 107.92, 105.59, 101.10, 50.65, 30.84, 21.69 (s, 2C), 9.36. HRMS: $(M + H)^+$ calcd for $C_{28}H_{26}F_2N_5O_5$, 550.1897; found, 550.1901.

*N-(4-((2-(Cyclopropanecarboxamido)pyridin-4-yl)oxy)-3-fluorophenyl)-3-(4-fluorophenyl)-1-isopropyl-2,4-dioxo-1,2,3,4-tetrahydropyrimidine-5-carboxamide (**13c**).* A mixture of **28c** (634 mg, 1.89 mmol), **17h** (553 mg, 1.89 mmol), HATU (863 mg, 2.27 mmol), and TEA (383 mg, 3.78 mmol) in DMF (18 mL) was stirred at RT overnight. The reaction mixture was poured into water (100 mL) and extracted with ethyl acetate (3 × 80 mL). The combined organic layer was washed with brine (5 × 100 mL), dried over anhydrous sodium sulfate, and evaporated under reduced pressure to give a residue. The residue was purified by silica gel chromatography (dichloromethane/methanol 98:2) to afford the title compound **13c** (778 mg, 73%) as a light yellow solid. $^1$H NMR (400 MHz, acetone-$d_6$): $\delta$ 11.07 (s, 1H), 9.77 (s, 1H), 8.66 (s, 1H), 8.14 (d, $J$ = 5.7 Hz, 1H), 8.05 (dd, $J$ = 13.0, 2.5 Hz, 1H), 7.84 (d, $J$ = 2.4 Hz, 1H), 7.52−7.40 (m, 3H), 7.36−7.25 (m, 3H), 6.64 (dd, $J$ = 5.7, 2.4 Hz, 1H), 4.93 (p, $J$ = 6.8 Hz, 1H), 2.02−1.94 (m, 1H), 1.50 (d, $J$ = 6.8 Hz, 6H), 0.91−0.77 (m, 4H). $^{13}$C NMR (126 MHz, $CDCl_3$): $\delta$ 172.58, 166.25, 162.94, 162.75 (d, $J$ = 249.4 Hz, 1C), 160.00, 154.21 (d, $J$ = 249.0 Hz, 1C), 153.63, 150.37, 148.76, 146.39, 136.88 (d, $J$ = 12.5 Hz, 1C), 136.52 (d, $J$ = 9.7 Hz, 1C), 130.20 (d, $J$ = 3.3 Hz, 1C), 129.93 (d, $J$ = 8.8 Hz, 2C), 123.47, 116.81 (d, $J$ = 23.1 Hz, 2C), 116.24 (d, $J$ = 3.4 Hz, 1C), 109.58 (d, $J$ = 23.3 Hz, 1C), 107.68, 105.45, 101.17, 50.55, 21.54 (s, 2C), 15.66, 8.31 (s, 2C). HRMS: $(M + H)^+$ calcd for $C_{29}H_{26}F_2N_5O_5$, 562.1897; found, 562.1894.

*N-(4-((2-(Cyclobutanecarboxamido)pyridin-4-yl)oxy)-3-fluorophenyl)-3-(4-fluorophenyl)-1-isopropyl-2,4-dioxo-1,2,3,4-tetrahydropyrimidine-5-carboxamide (**13d**).* A mixture of **32** (70 mg, 0.14 mmol), cyclobutanecarboxylic acid (142 mg, 1.41 mmol), HATU (647 mg, 1.7 mmol), and TEA (394 mg, 2.84 mmol) in DMF (1.5 mL) was stirred at 35 °C overnight. The reaction mixture was poured into water (15 mL) and extracted with ethyl acetate (3 × 15 mL). The combined organic layer was washed with brine (5 × 30 mL), dried over anhydrous sodium sulfate, and evaporated under reduced pressure to give a residue. The residue was purified by silica gel chromatography (dichloromethane/methanol 98:2) to afford the title compound **13d** (27 mg, 34%) as an off-white solid. $^1$H NMR (400 MHz, DMSO-$d_6$): $\delta$ 11.04 (s, 1H), 10.40 (s, 1H), 8.68 (s, 1H), 8.18 (d, $J$ = 5.8 Hz, 1H), 7.99 (dd, $J$ = 12.9, 2.5 Hz, 1H), 7.69 (d, $J$ = 2.4 Hz, 1H), 7.56−7.32 (m, 6H), 6.71 (dd, $J$ = 5.7, 2.4 Hz, 1H), 4.78 (p, $J$ = 6.8 Hz, 1H), 3.32−3.26 (m, 1H), 2.23−1.98 (m, 4H), 1.96−1.81 (m, 1H), 1.81−1.69 (m, 1H), 1.43 (d, $J$ = 6.7 Hz, 6H). $^{13}$C NMR (126 MHz, $CDCl_3$): $\delta$ 173.71, 166.39, 163.07, 162.89 (d, $J$ = 249.5 Hz, 1C), 160.12, 154.39 (d, $J$ = 249.0 Hz, 1C), 153.34, 150.48, 149.03, 146.49, 137.03 (d, $J$ = 12.5 Hz, 1C), 136.68 (d, $J$ = 9.6 Hz, 1C), 130.30 (d, $J$ = 3.3 Hz, 1C), 130.04 (d, $J$ = 8.8 Hz, 2C), 123.64, 116.96 (d, $J$ = 23.2 Hz, 2C), 116.37 (d, $J$ = 3.3 Hz, 1C), 109.74 (d, $J$ = 23.2 Hz, 1C), 107.97, 105.60, 100.95, 50.65, 40.92, 25.20 (s, 2C), 21.70 (s, 2C), 18.06. HRMS: $(M + H)^+$ calcd for $C_{30}H_{28}F_2N_5O_5$, 576.2053; found, 576.2049.

*N-(3-Fluoro-4-((2-(pyrrolidine-1-carboxamido)pyridin-4-yl)oxy)-phenyl)-3-(4-fluorophenyl)-1-isopropyl-2,4-dioxo-1,2,3,4-tetrahydropyrimidine-5-carboxamide (**13e**).* To a stirred solution of **32** (100 mg, 0.20 mmol) and TEA (41 mg, 0.41 mmol) in THF (7 mL) under argon was slowly added phenyl chloroformate (34 mg, 0.22 mmol) at 0 °C. The resulting mixture was warmed up to RT and stirred for 2 h. Then, pyrrolidine (43 mg, 0.60 mmol) was added, and the resulting mixture was stirred at RT overnight. The reaction mixture was poured into saturated aq ammonium chloride (50 mL) and extracted with dichloromethane (3 × 50 mL). The combined organic layer was washed with brine (100 mL), dried over anhydrous sodium sulfate, and evaporated under reduced pressure to give a residue. The residue was purified by silica gel chromatography (dichloromethane/methanol 99:1) to afford the title compound **13e** (29 mg, 24%) as a yellow solid. $^1$H NMR (400 MHz, acetone-$d_6$): $\delta$ 11.07 (s, 1H), 8.66 (s, 1H), 8.08−8.01 (m, 2H), 7.75 (d, $J$ = 2.4 Hz, 1H), 7.62 (s, 1H), 7.49−7.41 (m, 3H), 7.35−7.25 (m, 3H), 6.53 (dd, $J$ = 5.7, 2.4 Hz, 1H), 4.93 (p, $J$ = 6.8 Hz, 1H), 3.45 (s, 4H), 1.92 (s, 4H), 1.50 (d, $J$ = 6.8 Hz, 6H). $^{13}$C NMR (126 MHz, $CDCl_3$): $\delta$ 166.22, 163.04, 162.88 (d, $J$ = 249.7 Hz, 1C), 160.07, 154.67, 154.39 (d, $J$ = 249.2 Hz, 1C), 153.01, 150.48, 148.76, 146.45, 137.26 (d, $J$ = 12.5 Hz, 1C), 136.44 (d, $J$ = 9.5 Hz, 1C), 130.30, 130.04 (d, $J$ = 8.9 Hz, 2C), 123.60, 116.94 (d, $J$ = 23.1 Hz, 2C), 116.35 (d, $J$ = 3.5 Hz, 1C), 109.73 (d, $J$ = 23.3 Hz, 1C), 106.90, 105.62, 99.77,


https://doi.org/10.1021/acs.jmedchem.0c02093
J. Med. Chem. 2021, 64, 3956−3975

50.63 (s, 2C), 45.91 (s, 2C), 25.65, 21.68 (s, 2C). HRMS: $(M + H)^+$ calcd for $C_{30}H_{29}F_2N_6O_5$, 591.2162; found, 591.2162.

*N-(4-(2-Fluoro-4-(3-(4-fluorophenyl)-1-isopropyl-2,4-dioxo-1,2,3,4-tetrahydropyrimidine-5-carboxamido)phenoxy)pyridin-2-yl)morpholine-4-carboxamide (**13f**).* To a stirred solution of **32** (100 mg, 0.20 mmol) and TEA (41 mg, 0.41 mmol) in THF (7 mL) under argon was slowly added phenyl chloroformate (34 mg, 0.22 mmol) at 0 °C. The resulting mixture was warmed up to RT and stirred for 2 h. Then, morpholine (52 mg, 0.60 mmol) was added. The resulting mixture was stirred at RT overnight and further heated at 75 °C for 1.5 h. The reaction mixture was poured into saturated aq ammonium chloride (30 mL) and extracted with dichloromethane (3 × 30 mL). The combined organic layer was washed with brine (100 mL), dried over anhydrous sodium sulfate, and evaporated under reduced pressure to give a residue. The residue was purified by silica gel chromatography (dichloromethane/methanol 99:1) to afford the title compound **13f** (31 mg, 25.5%) as an off-white solid. $^1$H NMR (400 MHz, DMSO-$d_6$): $\delta$ 11.03 (s, 1H), 9.31 (s, 1H), 8.68 (d, $J$ = 1.0 Hz, 1H), 8.13 (d, $J$ = 5.7 Hz, 1H), 7.98 (dd, $J$ = 12.9, 2.4 Hz, 1H), 7.56−7.29 (m, 7H), 6.63 (dd, $J$ = 5.9, 2.3 Hz, 1H), 4.78 (p, $J$ = 6.8 Hz, 1H), 3.55 (t, $J$ = 4.7 Hz, 4H), 3.40 (t, $J$ = 4.8 Hz, 4H), 1.43 (d, $J$ = 6.7 Hz, 6H). $^{13}$C NMR (126 MHz, $CDCl_3$): $\delta$ 166.30, 163.06, 162.88 (d, $J$ = 249.4 Hz, 1C), 160.13, 154.56, 154.36 (d, $J$ = 249.1 Hz, 1C), 154.00, 150.47, 148.66, 146.48, 137.13 (d, $J$ = 12.5 Hz, 1C), 136.53 (d, $J$ = 9.6 Hz, 1C), 130.29 (d, $J$ = 3.3 Hz, 1C), 130.02 (d, $J$ = 8.8 Hz, 2C), 123.60, 116.94 (d, $J$ = 23.0 Hz, 2C), 116.38 (d, $J$ = 3.3 Hz, 1C), 109.75 (d, $J$ = 23.3 Hz, 1C), 107.06, 105.56, 100.32, 66.56 (s, 2C), 50.64 (s, 2C), 44.26, 21.67 (s, 2C). HRMS: $(M + H)^+$ calcd for $C_{30}H_{29}F_2N_6O_6$, 607.2111; found, 607.2113.

*4-((3-Chloropyridin-4-yl)oxy)aniline (**15**).* To a solution of 4-aminophenol (2.65 g, 24.3 mmol) in DMA (40 mL) was added potassium *tert*-butoxide (2.8 g, 24.9 mmol). The resulting mixture was stirred at RT for 0.5 h. Then, 4-bromo-3-chloropyridine (4.0 g, 20.7 mmol) was added, and the resulting mixture was stirred at 85 °C for 4 h. The reaction mixture was poured into water (400 mL) and extracted with ethyl acetate (4 × 100 mL). The combined organic layer was washed with brine (5 × 400 mL), dried over anhydrous sodium sulfate, and evaporated under reduced pressure to afford the title compound **15** (5.8 g, 100%) as a black solid. $^1$H NMR (300 MHz, DMSO-$d_6$): $\delta$ 8.65 (s, 1H), 8.31 (d, $J$ = 5.6 Hz, 1H), 6.86 (d, $J$ = 8.7 Hz, 2H), 6.74−6.51 (m, 3H), 5.21 (s, 2H). LC/MS (ESI, $m/z$): 265.0 $[M + H]^+$, 267.0 $[M + 2 + H]^+$.

*4-((3-(1-Methyl-1H-pyrazol-4-yl)pyridin-4-yl)oxy)aniline (**16**).* A mixture of **15** (1.2 g, 4.4 mmol), 1-methyl-4-pyrazole boronic acid pinacol ester (1.15 g, 5.55 mmol), and tetrakis(triphenylphosphine) palladium (0.5 g, 0.4 mmol) in 1,4-dioxane (20 mL)/water (4 mL) under argon was stirred at 90 °C for 9 h. After cooling, the resulting mixture was poured into saturated aq sodium bicarbonate (150 mL) and extracted with ethyl acetate (3 × 100 mL). The combined organic layer was washed with brine (200 mL), dried over anhydrous sodium sulfate, and evaporated under reduced pressure to give a residue. The residue was purified by silica gel chromatography (dichloromethane/methanol 97:3) to afford the title compound **16** (1.1 g, 97%) as a brown solid. $^1$H NMR (300 MHz, DMSO-$d_6$): $\delta$ 8.79 (s, 1H), 8.23 (s, 1H), 8.18 (d, $J$ = 5.6 Hz, 1H), 8.02−8.01 (m, 1H), 6.86 (d, $J$ = 8.7 Hz, 2H), 6.63 (d, $J$ = 8.8 Hz, 2H), 6.56 (d, $J$ = 5.7 Hz, 1H), 5.15 (s, 2H), 3.89 (s, 3H). LC/MS (ESI, $m/z$): 267.1 $[M + H]^+$.

*4-((2-Chloropyridin-4-yl)oxy)aniline (**19a**).* The compound was prepared from **18** and 4-aminophenol by following a similar procedure as described for **15**. Black solid, 96% yield. $^1$H NMR (300 MHz, DMSO-$d_6$): $\delta$ 8.23 (d, $J$ = 5.5 Hz, 1H), 6.91−6.80 (m, 4H), 6.67−6.58 (m, 2H), 5.20 (s, 2H). LC/MS (ESI, $m/z$): 221.1 $[M + H]^+$.

*4-((2-Chloropyridin-4-yl)oxy)-3-fluoroaniline (**19b**).* The compound was prepared from **18** and 4-amino-2-fluorophenol by following a similar procedure as described for **15**. Black solid, 100% yield. $^1$H NMR (300 MHz, DMSO-$d_6$): $\delta$ 8.26 (d, $J$ = 5.7 Hz, 1H), 7.01 (t, $J$ = 9.0 Hz, 1H), 6.96−6.88 (m, 2H), 6.55−6.39 (m, 2H), 5.53 (br s, 2H). LC/MS (ESI, $m/z$): 239.1 $[M + H]^+$.

*4-((2-Chloropyridin-4-yl)oxy)-2-fluoroaniline (**19c**).* The compound was prepared from **18** and 4-amino-3-fluorophenol by following a similar procedure as described for **15**. Beige solid, 83% yield. $^1$H NMR (400 MHz, DMSO-$d_6$): $\delta$ 8.25 (d, $J$ = 5.7 Hz, 1H), 7.02 (dd, $J$ = 11.9, 2.5 Hz, 1H), 6.94−6.87 (m, 2H), 6.87−6.75 (m, 2H), 5.23 (br s, 2H). LC/MS (ESI, $m/z$): 239.0 $[M + H]^+$.

*3-Chloro-4-((2-chloropyridin-4-yl)oxy)aniline (**19d**).* The compound was prepared from **18** and 4-amino-2-chlorophenol by following a similar procedure as described for **15**. Black solid, 97% yield. $^1$H NMR (400 MHz, $CDCl_3$): $\delta$ 8.19 (d, $J$ = 6.5 Hz, 1H), 6.92 (d, $J$ = 8.7 Hz, 1H), 6.78 (d, $J$ = 2.7 Hz, 1H), 6.75−6.70 (m, 2H), 6.59 (dd, $J$ = 8.7, 2.7 Hz, 1H), 3.84 (br s, 2H). LC/MS (ESI, $m/z$): 255.0 $[M + H]^+$.

*4-((2-Chloropyridin-4-yl)oxy)-3-methylaniline (**19e**).* The compound was prepared from **18** and 4-amino-2-methylphenol by following a similar procedure as described for **15**. $^1$H NMR (400 MHz, DMSO-$d_6$): $\delta$ 8.23 (d, $J$ = 6.0 Hz, 1H), 6.84−6.74 (m, 3H), 6.55−6.42 (m, 2H), 5.12 (s, 2H), 1.93 (s, 3H). LC/MS (ESI, $m/z$): 235.1 $[M + H]^+$.

*4-((2-Chloropyridin-4-yl)oxy)-3-methoxyaniline (**19f**).* The compound was prepared from **18** and 4-amino-2-methoxyphenol by following a similar procedure as described for **15**. Black solid, 91% yield. $^1$H NMR (400 MHz, $CDCl_3$): $\delta$ 8.17−8.13 (m, 1H), 6.84 (d, $J$ = 8.4 Hz, 1H), 6.74−6.71 (m, 2H), 6.33 (d, $J$ = 2.5 Hz, 1H), 6.25 (dd, $J$ = 8.4, 2.6 Hz, 1H), 3.78 (s, 2H), 3.70 (s, 3H). LC/MS (ESI, $m/z$): 251.1 $[M + H]^+$.

*4-((2-Chloropyridin-4-yl)oxy)-2,3-difluoroaniline (**19g**).* The compound was prepared from **18** and 4-amino-2,3-difluorophenol by following a similar procedure as described for **15**. Light brown solid, 94% yield. $^1$H NMR (400 MHz, DMSO-$d_6$): $\delta$ 8.87 (d, $J$ = 5.8 Hz, 1H), 7.65 (s, 1H), 7.60−7.48 (m, 2H), 7.22 (t, $J$ = 8.9 Hz, 1H), 6.21 (s, 2H). LC/MS (ESI, $m/z$): 257.0 $[M + H]^+$.

*4-((2-Chloropyridin-4-yl)oxy)-3,5-difluoroaniline (**19h**).* The compound was prepared from **18** and 4-amino-2,6-difluorophenol by following a similar procedure as described for **15**. Pale beige solid, 90% yield. $^1$H NMR (400 MHz, DMSO-$d_6$): $\delta$ 8.30 (d, $J$ = 5.8 Hz, 1H), 7.10 (d, $J$ = 2.3 Hz, 1H), 7.00 (dd, $J$ = 5.8, 2.4 Hz, 1H), 6.44−6.33 (m, 2H), 5.86 (br s, 2H). LC/MS (ESI, $m/z$): 257.0 $[M + H]^+$. LC/MS (ESI, $m/z$): 257.0 $[M + H]^+$.

*4-((2-(1-Methyl-1H-pyrazol-4-yl)pyridin-4-yl)oxy)aniline (**20a**).* The compound was prepared from **19a** and 1-methyl-4-pyrazole boronic acid pinacol ester by following a similar procedure as described for **16**. Light yellow solid, 75% yield. $^1$H NMR (300 MHz, DMSO-$d_6$): $\delta$ 8.30 (d, $J$ = 5.7 Hz, 1H), 8.21 (s, 1H), 7.96−7.88 (m, 1H), 7.12 (d, $J$ = 2.4 Hz, 1H), 6.90−6.80 (m, 2H), 6.67−6.57 (m, 2H), 6.53 (dd, $J$ = 5.7, 2.4 Hz, 1H), 5.15 (br s, 2H), 3.85 (s, 3H). LC/MS (ESI, $m/z$): 267.1 $[M + H]^+$.

*3-Fluoro-4-((2-(1-methyl-1H-pyrazol-4-yl)pyridin-4-yl)oxy)-aniline (**20b**).* The compound was prepared from **19b** and 1-methyl-4-pyrazole boronic acid pinacol ester by following a similar procedure as described for **16**. Brown solid, 100% yield. $^1$H NMR (300 MHz, $CDCl_3$): $\delta$ 8.32 (dd, $J$ = 5.8, 0.5 Hz, 1H), 7.86−7.81 (m, 2H), 6.95−6.87 (m, 2H), 6.57 (ddd, $J$ = 5.8, 2.5, 0.6 Hz, 1H), 6.48 (dd, $J$ = 11.9, 2.6 Hz, 1H), 6.42 (ddd, $J$ = 8.6, 2.7, 1.2 Hz, 1H), 3.88 (s, 3H), 2.64 (br s, 2H). LC/MS (ESI, $m/z$): 285.1 $[M + H]^+$.

*2-Fluoro-4-((2-(1-methyl-1H-pyrazol-4-yl)pyridin-4-yl)oxy)-aniline (**20c**).* The compound was prepared from **19c** and 1-methyl-4-pyrazole boronic acid pinacol ester by following a similar procedure as described for **16**. Dark brown solid, 94% yield. $^1$H NMR (400 MHz, DMSO-$d_6$): $\delta$ 8.32 (d, $J$ = 5.7 Hz, 1H), 8.23 (s, 1H), 7.94 (s, 1H), 7.14 (d, $J$ = 2.4 Hz, 1H), 6.97 (dd, $J$ = 11.9, 2.6 Hz, 1H), 6.88−6.73 (m, 2H), 6.58 (dd, $J$ = 5.8, 2.5 Hz, 1H), 5.17 (br s, 2H), 3.86 (s, 3H). LC/MS (ESI, $m/z$): 285.1 $[M + H]^+$.

*3-Chloro-4-((2-(1-methyl-1H-pyrazol-4-yl)pyridin-4-yl)oxy)-aniline (**20d**).* The compound was prepared from **19d** and 1-methyl-4-pyrazole boronic acid pinacol ester by following a similar procedure as described for **16**. Brown solid, 91% yield. $^1$H NMR (400 MHz, $CDCl_3$): $\delta$ 8.35 (d, $J$ = 5.8 Hz, 1H), 7.86 (d, $J$ = 4.2 Hz, 2H), 6.98−6.90 (m, 2H), 6.79 (d, $J$ = 2.7 Hz, 1H), 6.60 (dd, $J$ = 8.6, 2.7 Hz, 1H), 6.55 (dd, $J$ = 5.7, 2.4 Hz, 1H), 3.92 (s, 3H), 3.81 (br s, 2H). LC/MS (ESI, $m/z$): 301.1 $[M + H]^+$.

*3-Methyl-4-((2-(1-methyl-1H-pyrazol-4-yl)pyridin-4-yl)oxy)-aniline (**20e**).* The compound was prepared from **19e** and 1-methyl-4-pyrazole boronic acid pinacol ester by following a similar procedure as


https://doi.org/10.1021/acs.jmedchem.0c02093
J. Med. Chem. 2021, 64, 3956−3975

described for **16**. Tan solid, 71% yield. $^1$H NMR (400 MHz, DMSO-$d_6$): $\delta$ 8.29 (d, $J$ = 5.7 Hz, 1H), 8.21 (s, 1H), 7.92 (d, $J$ = 0.7 Hz, 1H), 7.10 (d, $J$ = 2.3 Hz, 1H), 6.76 (d, $J$ = 8.5 Hz, 1H), 6.53−6.42 (m, 3H), 5.06 (br s, 2H), 3.86 (s, 3H), 1.96 (s, 3H). LC/MS (ESI, $m/z$): 281.2 $[M + H]^+$.

*3-Methoxy-4-((2-(1-methyl-1H-pyrazol-4-yl)pyridin-4-yl)oxy)-aniline (**20f**).* The compound was prepared from **19f** and 1-methyl-4-pyrazole boronic acid pinacol ester by following a similar procedure as described for **16**. Dark brown solid, 64% yield. $^1$H NMR (400 MHz, $CDCl_3$): $\delta$ 8.32 (d, $J$ = 5.8 Hz, 1H), 7.88−7.84 (m, 2H), 6.95 (d, $J$ = 2.4 Hz, 1H), 6.89 (d, $J$ = 8.4 Hz, 1H), 6.57 (dd, $J$ = 5.8, 2.4 Hz, 1H), 6.37 (d, $J$ = 2.5 Hz, 1H), 6.29 (dd, $J$ = 8.4, 2.6 Hz, 1H), 3.93 (s, 3H), 3.74 (s, 3H), 3.72 (br s, 2H). LC/MS (ESI, $m/z$): 297.1 $[M + H]^+$.

*2,3-Difluoro-4-((2-(1-methyl-1H-pyrazol-4-yl)pyridin-4-yl)oxy)-aniline (**20g**).* The compound was prepared from **19g** and 1-methyl-4-pyrazole boronic acid pinacol ester by following a similar procedure as described for **16**. Light brown solid, 80% yield. $^1$H NMR (400 MHz, DMSO-$d_6$): $\delta$ 8.33 (d, $J$ = 5.7 Hz, 1H), 8.25 (s, 1H), 7.95 (s, 1H), 7.19 (d, $J$ = 1.9 Hz, 1H), 6.89 (t, $J$ = 8.6 Hz, 1H), 6.66−6.58 (m, 2H), 5.54 (br s, 2H), 3.85 (s, 3H). LC/MS (ESI, $m/z$): 303.1 $[M + H]^+$.

*3,5-Difluoro-4-((2-(1-methyl-1H-pyrazol-4-yl)pyridin-4-yl)oxy)-aniline (**20h**).* The compound was prepared from **19h** and 1-methyl-4-pyrazole boronic acid pinacol ester by following a similar procedure as described for **16**. Beige solid, 94% yield. $^1$H NMR (400 MHz, DMSO-$d_6$): $\delta$ 8.36 (d, $J$ = 5.7 Hz, 1H), 8.27 (s, 1H), 7.97 (s, 1H), 7.23 (d, $J$ = 2.5 Hz, 1H), 6.64 (dd, $J$ = 5.7, 2.5 Hz, 1H), 6.42−6.33 (m, 2H), 5.80 (br s, 2H), 3.86 (s, 3H). LC/MS (ESI, $m/z$): 303.1 $[M + H]^+$.

*4-((2-(1,3-Dimethyl-1H-pyrazol-4-yl)pyridin-4-yl)oxy)-3-fluoroaniline (**20i**).* The compound was prepared from **19b** and 1,3-dimethylpyrazole-4-boronic acid pinacol ester by following a similar procedure as described for **16**. Light brown solid, 72% yield. $^1$H NMR (400 MHz, DMSO-$d_6$): $\delta$ 8.37 (d, $J$ = 5.7 Hz, 1H), 8.10 (s, 1H), 7.14−6.86 (m, 2H), 6.68−6.33 (m, 3H), 5.47 (br s, 2H), 3.77 (s, 3H), 2.35 (s, 3H). LC/MS (ESI, $m/z$): 299.1 $[M + H]^+$.

*4-((2-(1-Cyclopropyl-1H-pyrazol-4-yl)pyridin-4-yl)oxy)-3-fluoroaniline (**20j**).* The compound was prepared from **19b** and 1-cyclopropylpyrazole-4-boronic acid pinacol ester by following a similar procedure as described for **16**. Pale yellow solid, 89% yield. $^1$H NMR (400 MHz, $CDCl_3$): $\delta$ 8.34 (d, $J$ = 5.8 Hz, 1H), 7.95 (s, 1H), 7.83 (s, 1H), 6.98−6.90 (m, 2H), 6.59 (dd, $J$ = 5.7, 2.4 Hz, 1H), 6.51 (dd, $J$ = 11.9, 2.7 Hz, 1H), 6.44 (ddd, $J$ = 8.6, 2.7, 1.2 Hz, 1H), 3.85 (br s, 2H), 3.64−3.58 (m, 1H), 1.15−1.10 (m, 2H), 1.05−0.99 (m, 2H). LC/MS (ESI, $m/z$): 311.1 $[M + H]^+$.

*1-(4-(4-(4-Amino-2-fluorophenoxy)pyridin-2-yl)-1H-pyrazol-1-yl)-2-methylpropan-2-ol (**20k**).* The compound was prepared from **19b** and 1-(2-hydroxy-2-methylpropyl)pyrazole-4-boronic acid pinacol ester by following a similar procedure as described for **16**. Pale pink solid, 51% yield. $^1$H NMR (400 MHz, DMSO-$d_6$): $\delta$ 8.33 (d, $J$ = 5.7 Hz, 1H), 8.18 (s, 1H), 7.96 (s, 1H), 7.17 (d, $J$ = 2.4 Hz, 1H), 7.00 (t, $J$ = 9.0 Hz, 1H), 6.59−6.40 (m, 3H), 5.46 (br s, 2H), 4.73 (s, 1H), 4.04 (s, 2H), 1.07 (s, 6H). LC/MS (ESI, $m/z$): 343.2 $[M + H]^+$.

*3-Fluoro-4-((2-(1-(2-(4-methylpiperazin-1-yl)ethyl)-1H-pyrazol-4-yl)pyridin-4-yl)oxy)aniline (**20l**).* The compound was prepared from **19b** and 1-(2-(4-methylpiperazin-1-yl)ethyl)pyrazole-4-boronic acid pinacol ester by following a similar procedure as described for **16**. Brown oil, 56% yield. $^1$H NMR (400 MHz, $CDCl_3$): $\delta$ 8.35 (d, $J$ = 5.7 Hz, 1H), 7.96 (s, 1H), 7.86 (s, 1H), 7.00−6.91 (m, 2H), 6.64−6.44 (m, 3H), 4.25 (t, $J$ = 6.7 Hz, 2H), 3.82 (s, 2H), 2.86 (t, $J$ = 6.7 Hz, 2H), 2.66−2.40 (m, 8H), 2.31 (s, 3H). LC/MS (ESI, $m/z$): 397.3 $[M + H]^+$.

*4-((2-(1H-Pyrazol-4-yl)pyridin-4-yl)oxy)-3-fluoroaniline (**20m**).* The compound was prepared from **19b** and 4-pyrazoleboronic acid pinacol ester by following a similar procedure as described for **16**. Tan solid, 44% yield. $^1$H NMR (400 MHz, DMSO-$d_6$): $\delta$ 13.06 (s, 1H), 8.36−8.28 (m, 2H), 8.01 (s, 1H), 7.26 (d, $J$ = 2.4 Hz, 1H), 7.00 (t, $J$ = 9.0 Hz, 1H), 6.56−6.47 (m, 2H), 6.46−6.39 (m, 1H), 5.46 (s, 2H). LC/MS (ESI, $m/z$): 271.1 $[M + H]^+$.

*2-Chloro-4-(2,5-difluoro-4-nitrophenoxy)pyridine (**22**).* To a solution of **21** (1.0 g, 7.7 mmol) in DMF (20 mL) was added potassium carbonate (1.28 g, 9.3 mmol) in one portion. After stirring at RT for 5 min, 1,2,4-trifluoro-5-nitrobenzene (1.37 g, 7.7 mmol) was slowly added with stirring. Then, the resulting mixture was stirred at RT for 0.5 h. The reaction mixture was poured into ice water (250 mL) and filtered. The filter cake was dried and purified by silica gel chromatography (petroleum ether/ethyl acetate 90:10) to afford the title compound **22** (1.24 g, 73%) as a yellow solid. $^1$H NMR (400 MHz, DMSO-$d_6$): $\delta$ 8.48 (dd, $J$ = 10.2, 7.1 Hz, 1H), 8.42 (d, $J$ = 5.7 Hz, 1H), 7.90 (dd, $J$ = 11.5, 6.7 Hz, 1H), 7.41 (d, $J$ = 2.3 Hz, 1H), 7.27 (dd, $J$ = 5.7, 2.3 Hz, 1H). LC/MS (ESI, $m/z$): 287.0 $[M + H]^+$.

*4-((2-Chloropyridin-4-yl)oxy)-2,5-difluoroaniline (**23**).* A mixture of **22** (2.00 g, 6.98 mmol) and stannous chloride (5.29 g, 27.91 mmol) in ethanol (144 mL) under argon was stirred at 80 °C for 8 h. Then, the reaction mixture was poured into saturated aq sodium bicarbonate (300 mL)/ethyl acetate (200 mL). The mixture was stirred and filtered. The filtrate was separated, and the aqueous layer was extracted with ethyl acetate (3 × 100 mL). The combined organic layer was washed with brine (2 × 300 mL), dried over anhydrous sodium sulfate, and evaporated under reduced pressure to give a residue. The residue was purified by silica gel chromatography (petroleum ether/ethyl acetate 90:10) to afford the title compound **23** (1.19 g, 66%) as a dark brown solid. $^1$H NMR (400 MHz, DMSO-$d_6$): $\delta$ 8.29 (d, $J$ = 5.8 Hz, 1H), 7.25 (dd, $J$ = 11.2, 7.4 Hz, 1H), 7.04 (d, $J$ = 2.3 Hz, 1H), 6.96 (dd, $J$ = 5.8, 2.3 Hz, 1H), 6.75 (dd, $J$ = 12.3, 8.3 Hz, 1H), 5.58 (br s, 2H). LC/MS (ESI, $m/z$): 257.0 $[M + H]^+$.

*2,5-Difluoro-4-((2-(1-methyl-1H-pyrazol-4-yl)pyridin-4-yl)oxy)-aniline (**24**).* The compound was prepared from **23** and 1-methyl-4-pyrazole boronic acid pinacol ester by following a similar procedure as described for **16**. Tan solid, 84% yield. $^1$H NMR (400 MHz, DMSO-$d_6$): $\delta$ 8.35 (d, $J$ = 5.7 Hz, 1H), 8.27 (s, 1H), 7.97 (d, $J$ = 0.8 Hz, 1H), 7.25−7.16 (m, 2H), 6.74 (dd, $J$ = 12.3, 8.3 Hz, 1H), 6.62 (dd, $J$ = 5.8, 2.4 Hz, 1H), 5.52 (br s, 2H), 3.87 (s, 3H). LC/MS (ESI, $m/z$): 303.1 $[M + H]^+$.

*N-(4-Chloropyridin-2-yl)acetamide (**26a**).* To a solution of **25** (1.30, 10 mmol) and TEA (4.0 g, 40 mmol) in dichloromethane (45 mL) was slowly added acetyl chloride (0.9 g, 12 mmol) at 0 °C. The resulting mixture was warmed up to RT and stirred for 17 h. The reaction mixture was poured into 200 mL of water and extracted with dichloromethane (3 × 100 mL). The combined organic layer was washed with brine (200 mL), dried over anhydrous sodium sulfate, and evaporated under reduced pressure to give a residue. The residue was purified by silica gel chromatography (petroleum ether/ethyl acetate 83:17) to afford the title compound **26a** (342 mg, 20%) as a rose red solid. $^1$H NMR (400 MHz, DMSO-$d_6$): $\delta$ 10.76 (s, 1H), 8.29 (d, $J$ = 5.4 Hz, 1H), 8.16 (d, $J$ = 2.0 Hz, 1H), 7.22 (dd, $J$ = 5.4, 2.0 Hz, 1H), 2.10 (s, 3H). LC/MS (ESI, $m/z$): 171.0 $[M + H]^+$.

*N-(4-Chloropyridin-2-yl)propionamide (**26b**).* The compound was prepared from **25** and propionyl chloride by following a similar procedure as described for **26a**. Light brown semi-solid, 14% yield. $^1$H NMR (400 MHz, DMSO-$d_6$): $\delta$ 10.70 (s, 1H), 8.29 (d, $J$ = 5.3 Hz, 1H), 8.19 (d, $J$ = 2.0 Hz, 1H), 7.21 (dd, $J$ = 5.4, 2.0 Hz, 1H), 2.40 (q, $J$ = 7.5 Hz, 2H), 1.06 (t, $J$ = 7.5 Hz, 3H). LC/MS (ESI, $m/z$): 185.1 $[M + H]^+$.

*N-(4-Chloropyridin-2-yl)cyclopropanecarboxamide (**26c**).* The compound was prepared from **25** and cyclopropanecarbonyl chloride by following a similar procedure as described for **26a**. Light yellow solid, 74% yield. $^1$H NMR (400 MHz, DMSO-$d_6$): $\delta$ 11.07 (s, 1H), 8.30 (d, $J$ = 5.3 Hz, 1H), 8.16 (d, $J$ = 1.9 Hz, 1H), 7.22 (dd, $J$ = 5.3, 2.0 Hz, 1H), 2.01 (p, $J$ = 6.2 Hz, 1H), 0.83 (d, $J$ = 6.2 Hz, 4H). LC/MS (ESI, $m/z$): 197.1 $[M + H]^+$.

*N-(4-(2-Fluoro-4-nitrophenoxy)pyridin-2-yl)acetamide (**27a**).* A mixture of **26a** (300 mg, 1.76 mmol) and 2-fluoro-4-nitrophenol (691 mg, 4.40 mmol) in chlorobenzene (4.4 mL) was heated in a sealed tube at 140 °C for 40 h. The resulting mixture was evaporated under reduced pressure to give a residue. The residue was purified by silica gel chromatography (dichloromethane/methanol 98:2) to afford the title compound **27a** (286 mg, 56%) as a brown solid. $^1$H NMR (400 MHz, DMSO-$d_6$): $\delta$ 10.71 (s, 1H), 8.44 (dd, $J$ = 10.5, 2.7 Hz, 1H), 8.29 (d, $J$ = 5.7 Hz, 1H), 8.24−8.16 (m, 1H), 7.78 (d, $J$ = 2.4 Hz, 1H), 7.61 (t, $J$ = 8.5 Hz, 1H), 6.84 (dd, $J$ = 5.8, 2.5 Hz, 1H), 2.06 (s, 3H). LC/MS (ESI, $m/z$): 292.1 $[M + H]^+$.

*N-(4-(2-Fluoro-4-nitrophenoxy)pyridin-2-yl)propionamide (**27b**).* The compound was prepared from **26b** and 2-fluoro-4-nitrophenol by


https://doi.org/10.1021/acs.jmedchem.0c02093
J. Med. Chem. 2021, 64, 3956−3975

following a similar procedure as described for **27a**. Yellow solid, 51% yield. $^1$H NMR (400 MHz, DMSO-$d_6$): $\delta$ 10.65 (s, 1H), 8.44 (dd, $J$ = 10.3, 2.7 Hz, 1H), 8.28 (d, $J$ = 5.8 Hz, 1H), 8.20 (d, $J$ = 9.1 Hz, 1H), 7.79 (d, $J$ = 2.3 Hz, 1H), 7.62 (t, $J$ = 8.5 Hz, 1H), 6.89−6.82 (m, 1H), 2.37 (q, $J$ = 7.6 Hz, 2H), 1.01 (t, $J$ = 7.5 Hz, 3H). LC/MS (ESI, $m/z$): 306.1 $[M + H]^+$.

*N-(4-(2-Fluoro-4-nitrophenoxy)pyridin-2-yl)-cyclopropanecarboxamide (**27c**).* The compound was prepared from **26c** and 2-fluoro-4-nitrophenol by following a similar procedure as described for **27a**. Yellow solid, 44% yield. $^1$H NMR (400 MHz, DMSO-$d_6$): $\delta$ 11.02 (s, 1H), 8.43 (dd, $J$ = 10.5, 2.7 Hz, 1H), 8.30 (d, $J$ = 5.7 Hz, 1H), 8.19 (ddd, $J$ = 9.0, 2.7, 1.4 Hz, 1H), 7.76 (d, $J$ = 2.4 Hz, 1H), 7.66−7.57 (m, 1H), 6.86 (dd, $J$ = 5.7, 2.4 Hz, 1H), 2.04−1.93 (m, 1H), 0.84−0.72 (m, 4H). LC/MS (ESI, $m/z$): 318.1 $[M + H]^+$.

*N-(4-(4-Amino-2-fluorophenoxy)pyridin-2-yl)acetamide (**28a**).* A mixture of **27a** (100 mg, 0.34 mmol), iron powder (96 mg, 1.72 mmol), and acetic acid (206 mg, 3.43 mmol) in ethyl acetate (1.8 mL)/water (0.36 mL) under argon was stirred at 80 °C for 2 h. The resulting mixture was filtered and washed with ethyl acetate (3 × 5 mL) and water (3 × 10 mL). The filtrate was extracted with ethyl acetate (3 × 20 mL). The combined organic layer was washed with saturated aq sodium bicarbonate (50 mL), dried over anhydrous sodium sulfate, and evaporated under reduced pressure to afford the title compound **28a** (86 mg, 96%) as a brown solid. $^1$H NMR (400 MHz, DMSO-$d_6$): $\delta$ 10.50 (s, 1H), 8.13 (d, $J$ = 5.7 Hz, 1H), 7.63−7.58 (m, 1H), 6.96 (t, $J$ = 9.0 Hz, 1H), 6.61 (dd, $J$ = 5.7, 2.5 Hz, 1H), 6.49 (dd, $J$ = 13.2, 2.6 Hz, 1H), 6.44−6.37 (m, 1H), 5.45 (br s, 2H), 2.03 (s, 3H). LC/MS (ESI, $m/z$): 262.1 $[M + H]^+$.

*N-(4-(4-Amino-2-fluorophenoxy)pyridin-2-yl)propionamide (**28b**).* The compound was prepared from **27b** by following a similar procedure as described for **28a**. Black solid, 96% yield. $^1$H NMR (400 MHz, DMSO-$d_6$): $\delta$ 10.43 (s, 1H), 8.13 (d, $J$ = 5.8 Hz, 1H), 7.62 (d, $J$ = 2.4 Hz, 1H), 6.96 (t, $J$ = 9.0 Hz, 1H), 6.62 (dd, $J$ = 5.7, 2.4 Hz, 1H), 6.50 (dd, $J$ = 13.2, 2.5 Hz, 1H), 6.41 (dd, $J$ = 8.9, 2.4 Hz, 1H), 5.46 (br s, 2H), 2.33 (q, $J$ = 7.5 Hz, 2H), 1.00 (t, $J$ = 7.5 Hz, 3H). LC/MS (ESI, $m/z$): 276.1 $[M + H]^+$.

*N-(4-(4-Amino-2-fluorophenoxy)pyridin-2-yl)-cyclopropanecarboxamide (**28c**).* The compound was prepared from **27c** by following a similar procedure as described for **28a**. Brown solid, 94% yield. $^1$H NMR (400 MHz, DMSO-$d_6$): $\delta$ 10.79 (s, 1H), 8.14 (d, $J$ = 5.8 Hz, 1H), 7.59 (d, $J$ = 2.4 Hz, 1H), 6.95 (t, $J$ = 9.0 Hz, 1H), 6.64 (dd, $J$ = 5.7, 2.4 Hz, 1H), 6.48 (dd, $J$ = 13.2, 2.5 Hz, 1H), 6.40 (dd, $J$ = 8.7, 2.2 Hz, 1H), 5.45 (br s, 2H), 1.98−1.91 (m, 1H), 0.80−0.73 (m, 4H). LC/MS (ESI, $m/z$): 288.1 $[M + H]^+$.

*4-(4-Amino-2-fluorophenoxy)picolinamide (**30**).* To a solution of 4-amino-2-fluorophenol (1.91 g, 15.0 mmol) in DMSO (19 mL) was added potassium *tert*-butoxide (1.795 g, 16 mmol). The resulting mixture was stirred at RT for 15 min. Then, 4-chloropicolinamide (1.57 g, 10.0 mmol) was added, and the resulting mixture was stirred at 80 °C for 1 h. The reaction mixture was poured into 0.5 M aq NaOH (38 mL) and stirred for 2 h. The precipitate was filtered and washed with water, and the cake was dried to afford the title compound **30** (2.14 g, 86%) as a brown solid. $^1$H NMR (400 MHz, DMSO-$d_6$): $\delta$ 8.49 (d, $J$ = 5.6 Hz, 1H), 8.12 (s, 1H), 7.72 (s, 1H), 7.34 (s, 1H), 7.15 (dd, $J$ = 5.6, 2.7 Hz, 1H), 7.02 (t, $J$ = 9.0 Hz, 1H), 6.53 (d, $J$ = 12.4 Hz, 1H), 6.44 (d, $J$ = 8.3 Hz, 1H), 5.53 (s, 2H). LC/MS (ESI, $m/z$): 248.1 $[M + H]^+$.

*N-(4-((2-Carbamoylpyridin-4-yl)oxy)-3-fluorophenyl)-3-(4-fluorophenyl)-1-isopropyl-2,4-dioxo-1,2,3,4-tetrahydropyrimidine-5-carboxamide (**31**).* The compound was prepared from **30** and **17h** by following a similar procedure as described for **13c**. Light yellow solid, 32% yield. $^1$H NMR (400 MHz, DMSO-$d_6$): $\delta$ 11.06 (s, 1H), 8.69 (s, 1H), 8.54 (d, $J$ = 5.6 Hz, 1H), 8.15 (d, $J$ = 1.8 Hz, 1H), 8.01 (dd, $J$ = 12.9, 2.5 Hz, 1H), 7.74 (d, $J$ = 1.6 Hz, 1H), 7.58−7.52 (m, 1H), 7.47−7.32 (m, 6H), 7.23 (dd, $J$ = 5.6, 2.7 Hz, 1H), 4.78 (p, $J$ = 6.7 Hz, 1H), 1.42 (d, $J$ = 6.8 Hz, 6H). LC/MS (ESI, $m/z$): 522.4 $[M + H]^+$.

*N-(4-((2-Aminopyridin-4-yl)oxy)-3-fluorophenyl)-3-(4-fluorophenyl)-1-isopropyl-2,4-dioxo-1,2,3,4-tetrahydropyrimidine-5-carboxamide (**32**).* To a mixture of **31** (170 mg, 0.33 mmol) in ethyl acetate (3 mL)/acetonitrile (3 mL)/water (1.5 mL) under argon was added iodobenzene diacetate (315 mg, 0.98 mmol) at 0 °C, and the resulting mixture was stirred at RT for 15 h. The reaction mixture was evaporated under reduced pressure to give a residue. The residue was purified by silica gel chromatography (dichloromethane/methanol 95:5) to afford the title compound **32** (57 mg, 36%) as a brown solid. $^1$H NMR (400 MHz, DMSO-$d_6$): $\delta$ 11.01 (s, 1H), 8.68 (s, 1H), 7.96 (dd, $J$ = 12.9, 2.0 Hz, 1H), 7.82 (d, $J$ = 6.0 Hz, 1H), 7.52−7.28 (m, 6H), 6.22 (dd, $J$ = 5.9, 2.5 Hz, 3H), 5.85 (d, $J$ = 1.8 Hz, 1H), 4.78 (p, $J$ = 6.8 Hz, 1H), 1.42 (d, $J$ = 6.8 Hz, 6H). LC/MS (ESI, $m/z$): 494.3 $[M + H]^+$.

**Kinase Inhibition Assay.** The activity of Axl and Met kinases was tested using ELISA as previously reported.[41] The $IC_{50}$ values were calculated from inhibition curves obtained from two separate experiments using a modified four-parameter logistic model. If the inhibitory rate is above 50% at the minimum tested compound concentration, the conclusion is that the $IC_{50}$ is lower than the tested minimum compound concentration. Moreover, if the inhibitory rate is below 50% at the maximum tested drug concentration, it shows that the $IC_{50}$ is higher than the tested maximum compound concentration. The kinase selectivity profile of **13c** (1000, 100, and 10 nmol/L) was screened against the abovementioned 40 other kinases by ELISA in local or radiometric protein kinase assays performed by Eurofins (UK) according to the manufacturer's instructions.

**Western Blot Analysis.** Cells were cultured under regular growth conditions to the exponential growth phase. The cells were then treated with the indicated dose of **13c** for 2 h and lysed in 1× sodium dodecyl sulfate (SDS) sample buffer. If Gas6 treatment was required, cells were serum-deprived for 24 h prior to 2 h of treatment with compounds and then stimulated with Gas6 for 15 min. The cell lysates were resolved by 10% SDS-PAGE and transferred to nitrocellulose membranes. Proteins were first probed with specific antibodies [against p-Axl(Y702), Axl, p-Met(Y1234/1235), p-Akt(S473), Akt, p-ERK1/2(T202/Y204), ERK1/2, $\beta$-actin, GAPDH (all from Cell Signaling Technology, USA), and Met (Santa Cruz Biotechnology, USA)], followed by a secondary horseradish peroxidase-conjugated antibody. Finally, immunoreactive proteins were detected using an enhanced chemiluminescence detection reagent (Thermo Fisher Scientific, USA).

**Cell Proliferation Assays.** Cells were seeded in 96-well plates at a low density in growth media. The next day, appropriate controls or designated concentrations of compounds were added to each well, and the cells were incubated for 72 h. Finally, cell proliferation was determined using a sulforhodamine B assay (SRB, Sigma-Aldrich, USA) or a cell counting kit (CCK-8, Dojindo, Japan) assay. The $IC_{50}$ values were calculated by concentration−response curve fitting using a SoftMax pro-based four-parameter method (SoftMax Pro Software, version 5.4.1).

**Cell Migration and Matrigel Invasion Assays.** For the migration assay, cells suspended in a serum-free medium ($1.5 \times 10^5$ cells per well) were seeded in 24-well transwell plates (pore size, 8 $\mu$m; Corning). The bottom chambers were filled with the serum-free medium supplemented with Gas6 (500 ng/mL) or cocultured cells, and appropriate controls or designated concentrations of compounds were added to both sides of the membrane. The cultures were maintained for 24 h, after which the nonmotile cells at the top of the filter were removed using a cotton swab. The migrating cells were fixed in paraformaldehyde (4%) and stained with crystal violet (0.1%) for 15 min at RT. For the invasion assay, cells were cultured in the top chambers containing Matrigel-coated membrane inserts. The ensuing procedure was identical to that of the migration assay. The assay was performed in triplicate. Images were obtained using an Olympus BX51 microscope.

**In Vivo Antitumor Activity Studies.** Animal procedures were approved by the Institutional Animal Care and Use Committee of the Shanghai Institute of Materia Medica (approval no. 2019-05-DJ-48). Cells at a density of 5−10 × $10^6$ in 200 $\mu$L were first implanted subcutaneously (sc) into the right flank of a nude mice and allowed to grow to 700−800 $mm^3$, which was defined as a well-developed tumor volume. The well-developed tumors were cut into 1.5 $mm^3$ fragments and transplanted sc into the right flank of nude mice. When the tumor volume reached 100−200 $mm^3$, the mice were randomly assigned into vehicle and treatment groups ($n$ = 6 in the treated group and $n$ = 12 in the vehicle group). The vehicle groups were given the vehicle alone, and the treatment groups received compounds at the indicated doses via po


https://doi.org/10.1021/acs.jmedchem.0c02093
J. Med. Chem. 2021, 64, 3956−3975

administration once daily for the indicated days. The tumor sizes were measured twice a week using a microcaliper. The tumor volume (TV) was calculated as TV = (length × width$^2$)/2. The percent (%) TGI rates were measured on the final day of the study for the compound-treated mice relative to the vehicle-treated mice and were calculated as $100 \times \{1 - [(TV_{\text{Treated Final day}} - TV_{\text{Treated Day 0}})/(TV_{\text{Vehicle Final day}} - TV_{\text{Vehicle Day 0}})]\}$. Significant differences between the treated versus the vehicle groups ($P \leq 0.05$) were determined using Student's *t*-test.

**Determination of Pharmacokinetic Parameters in Rats.** Male rats (SD rats, body-weight range of 330−390 g, $n = 3$) were administered compounds **12e** or **13c** by oral gavage at 3 mg/kg. A mixed solvent of 2.5% DMSO/97.5% [0.5% hydroxypropyl methyl cellulose (HPMC)] was used as the medium. Blood samples were collected at 0.25, 0.5, 1, 2, 4, 8, and 24 h after dosing. The plasma was separated by centrifugation, and the serum was collected in vials. The serum samples were frozen and stored at −70 °C before analysis. The test sample concentrations were determined by LC/MS. Animal procedures were performed according to the institutional ethical guidelines on animal care and approved by the Institute Animal Care and Use Committee at Shanghai Institute of Materia Medica (approval no. 2019-02-YY-07). The pharmacokinetic parameters were calculated using WinNonlin (version 6.4) software.

**Determination of Pharmacokinetic Parameters in Mice.** Male mice (ICR mice, body-weight range of 18−22 g, iv, $n = 3$, po, $n = 3$) were administered compound **13c** intravenously via the tail vein at 1 mg/kg or by oral gavage at 3 mg/kg. A mixed solvent of 5% DMSO/5% ethanol/40% PEG-300/50% (0.9% NaCl) was used as the injection medium. A mixed solvent of 2.5% DMSO/97.5% (0.5% HPMC) was used as the oral administration medium. For the po group, blood samples were collected at 0.25, 0.5, 1, 2, 4, 8, and 24 h after dosing. For the iv group, blood samples were collected at 0.25, 0.5, 0.75, 2, 4, 8, and 24 h after dosing. The plasma was separated by centrifugation, and the serum was collected in vials. The serum samples were frozen and stored at −70 °C before analysis. The test sample concentrations were determined by LC/MS. Animal procedures were performed according to the institutional ethical guidelines on animal care and approved by the Institute Animal Care and Use Committee at Shanghai Institute of Materia Medica (approval no. 2019-02-YY-08). The pharmacokinetic parameters were calculated using WinNonlin (version 6.4) software.

**Molecular Modeling.** The template Met crystal structure (PDB ID: 3F82) lacks residues Leu1225 to Ala1243. Thus, we decided to exclude this segment. The Axl/Met aligned sequences (as in Figure 2C) were taken out as two parts (part one: Val536 to Gly692 of Axl and Val1078 to Gly1224 of Met; part two: Lys710 to Leu799 of Axl and Lys1224 to Leu1333 of Met). We performed homology modeling of these two parts separately using the "Target/Template Alignment" method in SWISS-MODEL workspace via the ExPASy web server.[53] The two predicted structures were combined into one portion using Discovery Studio Visualizer (version 4.5.0, BIOVIA).

The docking study was performed using AutoDock (version 4.2) and AutoDockTools.[54] The predicted Axl DFG-out homology model was defined as the receptor. The docking site was defined using a grid box size of 35 × 61 × 60, spacing of 0.375 Å, and grid center of 0, 9, and 5. The Lamarckian genetic algorithm (GA) method was used in the docking protocol. Figures 2A, 4, and 5 were obtained from PyMOL (The PyMOL Molecular Graphics System, version 2.5, http://www.pymol.org) and Adobe Photoshop (version 2015.1.2).

## ■ ASSOCIATED CONTENT

### Supporting Information

The Supporting Information is available free of charge at https://pubs.acs.org/doi/10.1021/acs.jmedchem.0c02093.

Preparation of intermediate compounds, NMR spectra, and HPLC determination of compound **13c** (PDF)

Table of molecular formula strings (CSV)

Axl DFG-out homology model in the PDB format and docking poses for **10g** and **13c** (ZIP)

## ■ AUTHOR INFORMATION


### Corresponding Authors

**Jing Ai** − *Division of Antitumor Pharmacology, State Key Laboratory of Drug Research, Shanghai Institute of Materia Medica (SIMM), Chinese Academy of Sciences, Shanghai 201203, P. R. China; University of Chinese Academy of Sciences, Beijing 100049, P. R. China*; Phone: +86-21-50806600-2426; Email: jai@simm.ac.cn

**Wenhu Duan** − *Department of Medicinal Chemistry, Shanghai Institute of Materia Medica (SIMM), Chinese Academy of Sciences, Shanghai 201203, P. R. China; University of Chinese Academy of Sciences, Beijing 100049, P. R. China*; orcid.org/0000-0002-5084-6026; Phone: +86-21-50806032; Email: whduan@simm.ac.cn

### Authors

**Hefeng Zhang** − *Department of Medicinal Chemistry, Shanghai Institute of Materia Medica (SIMM), Chinese Academy of Sciences, Shanghai 201203, P. R. China; University of Chinese Academy of Sciences, Beijing 100049, P. R. China*

**Xia Peng** − *Division of Antitumor Pharmacology, State Key Laboratory of Drug Research, Shanghai Institute of Materia Medica (SIMM), Chinese Academy of Sciences, Shanghai 201203, P. R. China*

**Yang Dai** − *Division of Antitumor Pharmacology, State Key Laboratory of Drug Research, Shanghai Institute of Materia Medica (SIMM), Chinese Academy of Sciences, Shanghai 201203, P. R. China*

**Jingwei Shao** − *Department of Medicinal Chemistry, Shanghai Institute of Materia Medica (SIMM), Chinese Academy of Sciences, Shanghai 201203, P. R. China; University of Chinese Academy of Sciences, Beijing 100049, P. R. China*

**Yinchun Ji** − *Division of Antitumor Pharmacology, State Key Laboratory of Drug Research, Shanghai Institute of Materia Medica (SIMM), Chinese Academy of Sciences, Shanghai 201203, P. R. China*

**Yiming Sun** − *Division of Antitumor Pharmacology, State Key Laboratory of Drug Research, Shanghai Institute of Materia Medica (SIMM), Chinese Academy of Sciences, Shanghai 201203, P. R. China*

**Bo Liu** − *Division of Antitumor Pharmacology, State Key Laboratory of Drug Research, Shanghai Institute of Materia Medica (SIMM), Chinese Academy of Sciences, Shanghai 201203, P. R. China*

**Xu Cheng** − *Division of Antitumor Pharmacology, State Key Laboratory of Drug Research, Shanghai Institute of Materia Medica (SIMM), Chinese Academy of Sciences, Shanghai 201203, P. R. China; University of Chinese Academy of Sciences, Beijing 100049, P. R. China*

Complete contact information is available at: https://pubs.acs.org/10.1021/acs.jmedchem.0c02093

### Author Contributions

⊥H.Z. and X.P. contributed equally.


### Notes

The authors declare no competing financial interest.

## ■ ACKNOWLEDGMENTS

This work was supported by the funds from the Science and Technology Commission of Shanghai Municipality (no. 18431907100), the National Science & Technology Major Project "Key New Drug Creation and Manufacturing Program"

of China (no. 2018ZX09711002-011-016), the Natural Science Foundation of China for Innovation Research Group (no. 81821005), and the Collaborative Innovation Cluster Project of Shanghai Municipal Commission of Health and Family Planning (no. 2020CXJQ02).

## ■ ABBREVIATIONS

RTK, receptor tyrosine kinase; TAM, Tyro3, Axl, and Mer; Gas6, growth arrest specific protein 6; CML, chronic myeloid leukemia; EMT, epithelial-to-mesenchymal transition; DFG, aspartate−phenylalanine−glycine; AML, acute myeloid leukemia; SAR, atructure−activity relationship; ELISA, enzyme-linked immunosorbent assay; DHBA, dual hydrogen bond acceptor; SD, Sprague−Dawley; po, oral; iv, intravenous; ICR, Institute of Cancer Research; TGI, tumor growth inhibition; DMA, dimethylacetamide; RT, room temperature; HATU, *O*-(7-aza-1*H*-benzotriazol-1-yl)-*N*,*N*,*N*′,*N*′-tetramethyluronium hexafluorophosphate; TEA, triethylamine; DMF, *N*,*N*-dimethylformamide; DMSO, dimethyl sulfoxide; THF, tetrahydrofuran; TLC, thin-layer chromatography; LC, liquid chromatography; MS, mass spectrometry; SDS, sodium dodecyl sulfate; SRB, sulforhodamine B; MTT, thiazolyl blue tetrazolium bromide; sc, subcutaneously; TV, tumor volume; HPMC, hydroxypropyl methyl cellulose; GA, genetic algorithm

## ■ REFERENCES

(1) Varnum, B. C.; Young, C.; Elliott, G.; Garcia, A.; Bartley, T. D.; Fridell, Y.-W.; Hunt, R. W.; Trail, G.; Clogston, C.; Toso, R. J.; Yanagihara, D.; Bennett, L.; Sylber, M.; Merewether, L. A.; Tseng, A.; Escobar, E.; Liu, E. T.; Yamane, H. K. Axl receptor tyrosine kinase stimulated by the vitamin-K-dependent protein encoded by growth-arrest-specific gene 6. *Nature* **1995**, *373*, 623−626.

(2) Fridell, Y. W.; Jin, Y.; Quilliam, L. A.; Burchert, A.; McCloskey, P.; Spizz, G.; Varnum, B.; Der, C.; Liu, E. T. Differential activation of the Ras/extracellular-signal-regulated protein kinase pathway is responsible for the biological consequences induced by the Axl receptor tyrosine kinase. *Mol. Cell. Biol.* **1996**, *16*, 135−145.

(3) Sen, T.; Tong, P.; Diao, L.; Li, L.; Fan, Y.; Hoff, J.; Heymach, J. V.; Wang, J.; Byers, L. A. Targeting Axl and mTOR pathway overcomes primary and acquired resistance to Wee1 inhibition in small-cell lung cancer. *Clin. Cancer Res.* **2017**, *23*, 6239−6253.

(4) Linger, R. M. A.; Keating, A. K.; Earp, H. S.; Graham, D. K. TAM receptor tyrosine kinases: biologic functions, signaling, and potential therapeutic targeting in human cancer. In *Advances in Cancer Research, Vol. 100*; VandeWoude, G. F., Klein, G., Eds.; Elsevier Academic Press Inc.: San Diego, 2008; Vol. *100*, pp 35−83.

(5) Zhu, C. J.; Wei, Y. Q.; Wei, X. W. Axl receptor tyrosine kinase as a promising anti-cancer approach: functions, molecular mechanisms and clinical applications. *Mol. Cancer* **2019**, *18*, 153.

(6) Brown, M.; Black, J. R. M.; Sharma, R.; Stebbing, J.; Pinato, D. J. Gene of the month: Axl. *J. Clin. Pathol.* **2016**, *69*, 391−397.

(7) Ramjiawan, R. R.; Griffioen, A. W.; Duda, D. G. Anti-angiogenesis for cancer revisited: is there a role for combinations with immunotherapy? *Angiogenesis* **2017**, *20*, 185−204.

(8) O'bryan, J. P.; Frye, R. A.; Cogswell, P. C.; Neubauer, A.; Kitch, B.; Prokop, C.; Espinosa, R.; Lebeau, M. M.; Earp, H. S.; Liu, E. T. Axl, a transforming gene isolated from primary human myeloid leukemia cells, encodes a novel receptor tyrosine kinase. *Mol. Cell. Biol.* **1991**, *11*, 5016−5031.

(9) Myers, S. H.; Brunton, V. G.; Unciti-Broceta, A. Axl Inhibitors in cancer: a medicinal chemistry perspective. *J. Med. Chem.* **2016**, *59*, 3593−3608.

(10) Gjerdrum, C.; Tiron, C.; Hoiby, T.; Stefansson, I.; Haugen, H.; Sandal, T.; Collett, K.; Li, S.; McCormack, E.; Gjertsen, B. T.; Micklem, D. R.; Akslen, L. A.; Glackin, C.; Lorens, J. B. Axl is an essential epithelial-to-mesenchymal transition-induced regulator of breast cancer metastasis and patient survival. *Proc. Natl. Acad. Sci. U.S.A.* **2010**, *107*, 1124−1129.

(11) Okimoto, R. A.; Bivona, T. G. Axl receptor tyrosine kinase as a therapeutic target in NSCLC. *Lung Cancer* **2015**, *6*, 27−34.

(12) Reichl, P.; Dengler, M.; van Zijl, F.; Huber, H.; Führlinger, G.; Reichel, C.; Sieghart, W.; Peck-Radosavljevic, M.; Grubinger, M.; Mikulits, W. Axl activates autocrine transforming growth factor-beta signaling in hepatocellular carcinoma. *Hepatology* **2015**, *61*, 930−941.

(13) Koorstra, J.-B. M.; Karikari, C.; Feldmann, G.; Bisht, S.; Leal-Rojas, P.; Offerhaus, G. J. A.; Alvarez, H.; Maitra, A. The Axl receptor tyrosine kinase confers an adverse prognostic influence in pancreatic cancer and represents a new therapeutic target. *Cancer Biol. Ther.* **2009**, *8*, 618−626.

(14) Yu, H.; Liu, R.; Ma, B.; Li, X.; Yen, H.-y.; Zhou, Y.; Krasnoperov, V.; Xia, Z.; Zhang, X.; Bove, A. M.; Buscarini, M.; Parekh, D.; Gill, I. S.; Liao, Q.; Tretiakova, M.; Quinn, D.; Zhao, J.; Gill, P. S. Axl receptor tyrosine kinase is a potential therapeutic target in renal cell carcinoma. *Br. J. Cancer* **2015**, *113*, 616−625.

(15) Rankin, E. B.; Fuh, K. C.; Taylor, T. E.; Krieg, A. J.; Musser, M.; Yuan, J.; Wei, K.; Kuo, C. J.; Longacre, T. A.; Giaccia, A. J. Axl is an essential factor and therapeutic target for metastatic ovarian cancer. *Cancer Res.* **2010**, *70*, 7570−7579.

(16) Zhang, S.; Xu, X. S.; Yang, J. X.; Guo, J. H.; Chao, T. F.; Tong, Y. The prognostic role of Gas6/Axl axis in solid malignancies: a meta-analysis and literature review. *OncoTargets Ther.* **2018**, *11*, 509−519.

(17) Brand, T. M.; Iida, M.; Stein, A. P.; Corrigan, K. L.; Braverman, C. M.; Luthar, N.; Toulany, M.; Gill, P. S.; Salgia, R.; Kimple, R. J.; Wheeler, D. L. Axl mediates resistance to cetuximab therapy. *Cancer Res.* **2014**, *74*, 5152−5164.

(18) Elkabets, M.; Pazarentzos, E.; Juric, D.; Sheng, Q.; Pelossof, R. A.; Brook, S.; Benzaken, A. O.; Rodon, J.; Morse, N.; Yan, J. J.; Liu, M.; Das, R.; Chen, Y.; Tam, A.; Wang, H.; Liang, J.; Gurski, J. M.; Kerr, D. A.; Rosell, R.; Teixidó, C.; Huang, A.; Ghossein, R. A.; Rosen, N.; Bivona, T. G.; Scaltriti, M.; Baselga, J. Axl mediates resistance to PI3Kalpha inhibition by activating the EGFR/PKC/mTOR axis in head and neck and esophageal squamous cell carcinomas. *Cancer Cell* **2015**, *27*, 533−546.

(19) Bansal, N.; Mishra, P. J.; Stein, M.; DiPaola, R. S.; Bertino, J. R. Axl receptor tyrosine kinase is up-regulated in metformin resistant prostate cancer cells. *Oncotarget* **2015**, *6*, 15321−15331.

(20) Lin, J.-Z.; Wang, Z.-J.; De, W.; Zheng, M.; Xu, W.-Z.; Wu, H.-F.; Armstrong, A.; Zhu, J.-G. Targeting Axl overcomes resistance to docetaxel therapy in advanced prostate cancer. *Oncotarget* **2017**, *8*, 41064−41077.

(21) Hugo, W.; Zaretsky, J. M.; Sun, L.; Song, C.; Moreno, B. H.; Hu-Lieskovan, S.; Berent-Maoz, B.; Pang, J.; Chmielowski, B.; Cherry, G.; Seja, E.; Lomeli, S.; Kong, X.; Kelley, M. C.; Sosman, J. A.; Johnson, D. B.; Ribas, A.; Lo, R. S. Genomic and transcriptomic features of response to anti-PD-1 therapy in metastatic melanoma. *Cell* **2016**, *165*, 35−44.

(22) Paul, M. D.; Hristova, K. The RTK interactome: overview and perspective on RTK heterointeractions. *Chem. Rev.* **2019**, *119*, 5881−5921.

(23) Salian-Mehta, S.; Xu, M.; Wierman, M. E. Axl and Met crosstalk to promote gonadotropin releasing hormone (GnRH) neuronal cell migration and survival. *Mol. Cell. Endocrinol.* **2013**, *374*, 92−100.

(24) Belfiore, A.; Busico, A.; Bozzi, F.; Brich, S.; Dallera, E.; Conca, E.; Capone, I.; Gloghini, A.; Volpi, C. C.; Cabras, A. D.; Pilotti, S.; Baratti, D.; Guaglio, M.; Deraco, M.; Kusamura, S.; Perrone, F. Molecular signatures for combined targeted treatments in diffuse malignant peritoneal mesothelioma. *Int. J. Mol. Sci.* **2019**, *20*, 13.

(25) Mak, M. P.; Tong, P.; Diao, L.; Cardnell, R. J.; Gibbons, D. L.; William, W. N.; Skoulidis, F.; Parra, E. R.; Rodriguez-Canales, J.; Wistuba, I. I.; Heymach, J. V.; Weinstein, J. N.; Coombes, K. R.; Wang, J.; Byers, L. A. A patient-derived, pan-cancer EMT signature identifies global molecular alterations and immune target enrichment following epithelial-to-mesenchymal transition. *Clin. Cancer Res.* **2016**, *22*, 609−620.

(26) Byers, L. A.; Diao, L.; Wang, J.; Saintigny, P.; Girard, L.; Peyton, M.; Shen, L.; Fan, Y.; Giri, U.; Tumula, P. K.; Nilsson, M. B.; Gudikote,



https://doi.org/10.1021/acs.jmedchem.0c02093
J. Med. Chem. 2021, 64, 3956−3975

J.; Tran, H.; Cardnell, R. J. G.; Bearss, D. J.; Warner, S. L.; Foulks, J. M.; Kanner, S. B.; Gandhi, V.; Krett, N.; Rosen, S. T.; Kim, E. S.; Herbst, R. S.; Blumenschein, G. R.; Lee, J. J.; Lippman, S. M.; Ang, K. K.; Mills, G. B.; Hong, W. K.; Weinstein, J. N.; Wistuba, I. I.; Coombes, K. R.; Minna, J. D.; Heymach, J. V. An epithelial-mesenchymal transition gene signature predicts resistance to EGFR and PI3K inhibitors and identifies Axl as a therapeutic target for overcoming EGFR inhibitor resistance. *Clin. Cancer Res.* **2013**, *19*, 279−290.

(27) Nakamichi, S.; Seike, M.; Miyanaga, A.; Chiba, M.; Zou, F.; Takahashi, A.; Ishikawa, A.; Kunugi, S.; Noro, R.; Kubota, K.; Gemma, A. Overcoming drug-tolerant cancer cell subpopulations showing Axl activation and epithelial-mesenchymal transition is critical in conquering ALK-positive lung cancer. *Oncotarget* **2018**, *9*, 27242−27255.

(28) Tanaka, M.; Siemann, D. W. Gas6/Axl signaling pathway in the tumor immune microenvironment. *Cancers* **2020**, *12*, 1850.

(29) Wang, C.; Jin, H.; Wang, N.; Fan, S.; Wang, Y.; Zhang, Y.; Wei, L.; Tao, X.; Gu, D.; Zhao, F.; Fang, J.; Yao, M.; Qin, W. Gas6/Axl axis contributes to chemoresistance and metastasis in breast cancer through Akt/GSK-3$\beta$/$\beta$-catenin signaling. *Theranostics* **2016**, *6*, 1205−1219.

(30) Aguilera, T. A.; Rafat, M.; Castellini, L.; Shehade, H.; Kariolis, M. S.; Hui, A. B.-Y.; Stehr, H.; von Eyben, R.; Jiang, D.; Ellies, L. G.; Koong, A. C.; Diehn, M.; Rankin, E. B.; Graves, E. E.; Giaccia, A. J. Reprogramming the immunological microenvironment through radiation and targeting Axl. *Nat. Commun.* **2016**, *7*, 13898.

(31) Mori, M.; Kaneko, N.; Ueno, Y.; Tanaka, R.; Cho, K.; Saito, R.; Kondoh, Y.; Shimada, I.; Kuromitsu, S. ASP2215, a novel FLT3/Axl inhibitor: preclinical evaluation in acute myeloid leukemia (AML). *J. Clin. Oncol.* **2014**, *32*, 7070.

(32) Holland, S. J.; Pan, A.; Franci, C.; Hu, Y.; Chang, B.; Li, W.; Duan, M.; Torneros, A.; Yu, J.; Heckrodt, T. J.; Zhang, J.; Ding, P.; Apatira, A.; Chua, J.; Brandt, R.; Pine, P.; Goff, D.; Singh, R.; Payan, D. G.; Hitoshi, Y. R428, a selective small molecule inhibitor of axl kinase, blocks tumor spread and prolongs survival in models of metastatic breast cancer. *Cancer Res.* **2010**, *70*, 1544−1554.

(33) Hart, C. D.; De Boer, R. H. Profile of cabozantinib and its potential in the treatment of advanced medullary thyroid cancer. *OncoTargets Ther.* **2013**, *6*, 1−7.

(34) You, W.-K.; Sennino, B.; Williamson, C. W.; Falcón, B.; Hashizume, H.; Yao, L.-C.; Aftab, D. T.; McDonald, D. M. VEGF and c-Met blockade amplify angiogenesis inhibition in pancreatic islet cancer. *Cancer Res.* **2011**, *71*, 4758−4768.

(35) Qian, F.; Engst, S.; Yamaguchi, K.; Yu, P.; Won, K.-A.; Mock, L.; Lou, T.; Tan, J.; Li, C.; Tam, D.; Lougheed, J.; Yakes, F. M.; Bentzien, F.; Xu, W.; Zaks, T.; Wooster, R.; Greshock, J.; Joly, A. H. Inhibition of tumor cell growth, invasion, and metastasis by EXEL-2880 (XL880, GSK1363089), a novel inhibitor of HGF and VEGF receptor tyrosine kinases. *Cancer Res.* **2009**, *69*, 8009−8016.

(36) Xi, N. Substituted quinoline compounds and methods of use. U.S. Patent 20,120,219,522 A1, 2012.

(37) Yan, S. B.; Peek, V. L.; Ajamie, R.; Buchanan, S. G.; Graff, J. R.; Heidler, S. A.; Hui, Y.-H.; Huss, K. L.; Konicek, B. W.; Manro, J. R.; Shih, C.; Stewart, J. A.; Stewart, T. R.; Stout, S. L.; Uhlik, M. T.; Um, S. L.; Wang, Y.; Wu, W.; Yan, L.; Yang, W. J.; Zhong, B.; Walgren, R. A. LY2801653 is an orally bioavailable multi-kinase inhibitor with potent activity against Met, Mst1r, and other oncoproteins, and displays anti-tumor activities in mouse xenograft models. *Invest. New Drugs* **2013**, *31*, 833−844.

(38) Angeles, T. S.; Ator, M. A.; Cheng, M. M.; Dorsey, B.; Hudkins, R. L.; Ruggeri, B. A. Methods of treating various cancers using an Axl/cMet inhibitor alone or in combination with other agents. WO 2015017607 A2, 2015.

(39) Tan, L.; Zhang, Z.; Gao, D.; Luo, J.; Tu, Z.-C.; Li, Z.; Peng, L.; Ren, X.; Ding, K. 4-oxo-1,4-dihydroquinoline-3-carboxamide derivatives as new Axl kinase inhibitors. *J. Med. Chem.* **2016**, *59*, 6807−6825.

(40) Zheng, B.; Guo, H.; Ma, N.; Ni, Y.; Xu, J.; Li, L.; Hao, P.; Ding, K.; Li, Z. Cell- and tissue-based proteome profiling and bioimaging with probes derived from a potent Axl kinase inhibitor. *Chem.−Asian J.* **2018**, *13*, 2601−2605.

(41) Yan, W.; Wang, X.; Dai, Y.; Zhao, B.; Yang, X.; Fan, J.; Gao, Y.; Meng, F.; Wang, Y.; Luo, C.; Ai, J.; Geng, M.; Duan, W. Discovery of 3-(5′-Substituted)-benzimidazole-5-(1-(3,5-dichloropyridin-4-yl)-ethoxy)-1H-indazoles as potent fibroblast growth factor receptor inhibitors: design, synthesis, and biological evaluation. *J. Med. Chem.* **2016**, *59*, 6690−6708.

(42) Mori, M.; Kaneko, N.; Ueno, Y.; Yamada, M.; Tanaka, R.; Saito, R.; Shimada, I.; Mori, K.; Kuromitsu, S. Gilteritinib, a FLT3/Axl inhibitor, shows antileukemic activity in mouse models of FLT3 mutated acute myeloid leukemia. *Invest. New Drugs* **2017**, *35*, 556−565.

(43) Schultz-Fademrecht, C.; Klebl, B.; Choidas, A.; Koch, U.; Eickhoff, J.; Wolf, A.; Ullrich, A. Preparation of quinoline carboxamide compounds as Axl inhibitors. WO 2012028332 A1, 2012.

(44) Barvian, M. R.; Panek, R. L.; Lu, G. H.; Kraker, A. J.; Amar, A.; Hartl, B.; Hamby, J. M.; Showalter, H. D. H. 1-oxo-3-aryl-1H-indene-2-carboxylic acid derivatives as selective inhibitors of fibroblast growth factor receptor-1 tyrosine kinase. *Bioorg. Med. Chem. Lett.* **1997**, *7*, 2903−2908.

(45) Kovacs, P. R.; Patel, K. M.; Selby, T. P.; Smith, B. T.; Taggi, A. E. Herbicidal pyrimidone derivatives. WO 2011031658 A1, 2011.

(46) Inukai, T.; Takeuchi, J.; Yasuhiro, T. Quinoline derivatives. WO 2016104617 A1, 2016.

(47) Inukai, T.; Takeuchi, J.; Yasuhiro, T. Quinoline derivative. WO 2015012298 A1, 2015.

(48) Tang, Q.; Duan, Y.; Xiong, H.; Chen, T.; Xiao, Z.; Wang, L.; Xiao, Y.; Huang, S.; Xiong, Y.; Zhu, W.; Gong, P.; Zheng, P. Synthesis and antiproliferative activity of 6,7-disubstituted-4-phenoxyquinoline derivatives bearing the 1,8-naphthyridin-2-one moiety. *Eur. J. Med. Chem.* **2018**, *158*, 201−213.

(49) Dandu, R.; Hudkins, R. L.; Josef, K. A.; Prouty, C. P.; Tripathy, R. Uracil derivatives as axl and c-met kinase inhibitors. WO2013074633A1, 2013.

(50) Schroeder, G. M.; An, Y.; Cai, Z.-W.; Chen, X.-T.; Clark, C.; Cornelius, L. A. M.; Dai, J.; Gullo-Brown, J.; Gupta, A.; Henley, B.; Hunt, J. T.; Jeyaseelan, R.; Kamath, A.; Kim, K.; Lippy, J.; Lombardo, L. J.; Manne, V.; Oppenheimer, S.; Sack, J. S.; Schmidt, R. J.; Shen, G.; Stefanski, K.; Tokarski, J. S.; Trainor, G. L.; Wautlet, B. S.; Wei, D.; Williams, D. K.; Zhang, Y.; Zhang, Y.; Fargnoli, J.; Borzilleri, R. M. Discovery of N-(4-(2-amino-3-chloropyridin-4-yloxy)-3-fluorophenyl)-4-ethoxy-1-(4-fluorophenyl)-2-oxo-1,2-dihydropyridine-3-carboxamide (BMS-777607), a selective and orally efficacious inhibitor of the Met kinase superfamily. *J. Med. Chem.* **2009**, *52*, 1251−1254.

(51) Guengerich, F. P.; Macdonald, T. L. Chemical mechanisms of catalysis by cytochromes P-450: a unified view. *Acc. Chem. Res.* **1984**, *17*, 9−16.

(52) Zou, H. Y.; Li, Q.; Lee, J. H.; Arango, M. E.; McDonnell, S. R.; Yamazaki, S.; Koudriakova, T. B.; Alton, G.; Cui, J. J.; Kung, P.-P.; Nambu, M. D.; Los, G.; Bender, S. L.; Mroczkowski, B.; Christensen, J. G. An orally available small-molecule inhibitor of c-Met, PF-2341066, exhibits cytoreductive antitumor efficacy through antiproliferative and antiangiogenic mechanisms. *Cancer Res.* **2007**, *67*, 4408−4417.

(53) Waterhouse, A.; Bertoni, M.; Bienert, S.; Studer, G.; Tauriello, G.; Gumienny, R.; Heer, F. T.; de Beer, T. A. P.; Rempfer, C.; Bordoli, L.; Lepore, R.; Schwede, T. SWISS-MODEL: homology modelling of protein structures and complexes. *Nucleic Acids Res.* **2018**, *46*, W296−W303.

(54) Morris, G. M.; Huey, R.; Lindstrom, W.; Sanner, M. F.; Belew, R. K.; Goodsell, D. S.; Olson, A. J. AutoDock4 and AutoDockTools4: automated docking with selective receptor flexibility. *J. Comput. Chem.* **2009**, *30*, 2785−2791.



https://doi.org/10.1021/acs.jmedchem.0c02093
J. Med. Chem. 2021, 64, 3956−3975